NASA TM X-1071

A LOW-SPEED LONGITUDINAL STABILITY IMPROVEMENT STUDY ON A HIGHLY SWEPT SUPERSONIC TRANSPORT CONFIGURATION

By William P. Henderson

Langley Research Center
Langley Station, Hampton, Va.

NATIONAL AERONAUTICS AND SPACE ADMINISTRATION

L-4254

A LOW-SPEED LONGITUDINAL STABILITY IMPROVEMENT STUDY ON A HIGHLY SWEPT SUPERSONIC TRANSPORT CONFIGURATION*

By William P. Henderson
Langley Research Center

SUMMARY

13245

A wind-tunnel investigation was conducted to determine the effects of wing and outboard-tail modifications on the longitudinal aerodynamic characteristics of a highly swept, blended wing-body, supersonic commercial air transport (SCAT) configuration. The modifications examined in this investigation included wing trailing-edge planform changes, leading-edge chord extensions, wing upper-surface leading-edge flaps, wing-body juncture slots, and various arrangements of the outboard tail surfaces. The investigation was made at a Mach number of 0.186 and at angles of attack from -5° to 22°. The test Reynolds number per foot was 1.35×10^{6}.

The results indicate that modifications and leading-edge devices applied individually to the wing or outboard tail surfaces of this configuration generally produced small improvements in the pitching-moment variation with lift coefficient. When combinations of these modifications and leading-edge devices were employed, nearly linear variations of pitching-moment coefficient with lift coefficient were obtained.

Applying these modifications and leading-edge devices to the configurations usually resulted in reductions in the lift coefficient at a given angle of attack and in the maximum lift-drag ratio.

Author 7

INTRODUCTION

The National Aeronautics and Space Administration is studying the aerodynamic characteristics of configurations that may be suitable for use as supersonic transport configurations. One of these configurations, which is the subject of the present investigation, is a modified version of the SCAT 15 configuration. This configuration in its original form (as shown in refs. 1 to 4) combined a fixed wing of 75° leading-edge sweep with auxiliary wing panels whose sweep could be varied from 25° to 75°; at 75° the auxiliary wing panel became an integral part of the fixed wing. For reasons such as wing weight and aeroelasticity problems associated with the auxiliary wing panel (ref. 5), this

variable-sweep configuration was considered impractical. However, the aerodynamic characteristics for this configuration with the auxiliary wing panels fully swept back indicated good performance potential at supersonic speeds. In view of these results the auxiliary wing panels were eliminated and the configuration was treated as though it employed a highly sweptback fixed wing. Even this fixed-wing configuration exhibited certain deficiencies, one of which was the loss of longitudinal stability at moderate lift coefficients at subsonic speeds; this loss can be seen from the data presented in reference 4. An investigation was therefore conducted in the Langley high-speed 7- by 10-foot tunnel to examine several possible ways of improving the low-speed longitudinal stability characteristics, and the purpose of this paper is to present the results obtained during this investigation.

The modifications examined in this investigation included wing trailing-edge planform changes, leading-edge chord extensions, wing upper-surface leading-edge flaps, wing-body juncture slots, and various arrangements of the outboard tail surfaces. The study was conducted at a Mach number of 0.186 and at angles of attack from -5° to 22°. The test Reynolds number per foot was 1.35×10^{6}.

SYMBOLS

The forces and moments are presented about the wind-axis system. The coefficients for each wing are nondimensionalized with respect to the planform characteristics of that particular wing. The reference dimensions are tabulated in table I for each wing planform. The moment center for all wing planforms is located 65.00 inches behind the nose of the original fuselage as shown in figure 1.

b reference span, 32.00 in.

$\bar{c}$ mean geometric chord, in.

C_D drag coefficient, $\frac{\text{Drag}}{qS}$

C_L lift coefficient, $\frac{\text{Lift}}{qS}$

C_m pitching-moment coefficient, $\frac{\text{Pitching moment}}{qS\bar{c}}$

h height of wing leading-edge flap (perpendicular distance from top of flap to wing surface), in.

L/D lift-drag ratio

q free-stream dynamic pressure, lb/sq ft

S reference area (excluding outboard-tail area), sq ft

x distance along fuselage from fuselage base (positive forward of base), in.

y distance measured along wing span from plane of symmetry, in.

α angle of attack, deg

MODEL

Basic configuration.- A drawing of the basic configuration of this investigation is shown in figure 1. This configuration employs a highly sweptback, twisted and cambered wing (designated wing 1) blended with a fuselage. Twin vertical tails are located at the wing tips in combination with horizontal tail surfaces located outboard of the vertical tail surfaces. A more complete description of the geometric characteristics of the model is given in references 3 and 4. Also shown in figure 1 is the modified fuselage nose which was used throughout most of this investigation.

Modified wings.- The basic wing was modified to give wings 2 to 10 by the addition of trailing-edge extensions made of 1/16-inch-thick flat plate. Drawings of the planforms of wings 2 to 10 are shown in figures 2 and 3. Ordinates for the trailing edges of the wings that do not have straight trailing edges are presented in table II.

Leading-edge chord extensions.- Two types of wing leading-edge chord extensions (designated chord extensions 1 and 2) were investigated. (See fig. 4.) Chord extension 1 extended from 71.5 percent of the wing semispan to the tip of the outboard horizontal tail surfaces and had an incidence angle of 0°. (In this case, the wing semispan included the horizontal tail surfaces.) Chord extension 2 was placed only on the outboard horizontal tail surfaces and had an incidence angle of -30° with respect to the outboard-tail chord plane.

Leading-edge flaps.- Figure 5 shows a drawing of the wing upper-surface leading-edge flaps investigated. The leading-edge flap extended along the wing leading edge from the fuselage out to the vertical tails, and simulated flaps that would be raised from the upper surface of the wing. Two variations (A and B) of this leading-edge flap were investigated and are shown in figure 5 as sections perpendicular to the wing leading edge. The height h of the wing leading-edge flap B varied from 0.25 inch to 0.80 inch.

Tail surfaces.- In addition to the original position (position 1) of the outboard horizontal tail surfaces, two other positions were investigated. In these two alternate positions, the horizontal tail surfaces were located at the tip of the vertical tail surfaces with the horizontal tails placed outboard (position 2) and inboard (position 3) of the vertical tails. These tail positions are shown in figure 6. In another arrangement, the outboard vertical and horizontal tail surfaces were replaced by T-tails. The horizontal tail

surfaces had the same total planform area as did the horizontal tails in the original position. (See fig. 7.)

Slot configurations.- The section of the wing near the juncture of the wing leading edge and the fuselage was removed and replaced by a section constructed of wood. This wooden section had nearly the same planform and airfoil section as the original metal section had, and it was used so that slots could easily be cut through the wing. Three slots (designated slot configurations A, B, and C) were cut, as shown in figure 8, completely through the wing in order to allow air to flow through the wing from the bottom surface to the upper surface. Each slot had a 45° slope on each of the spanwise edges.

TESTS AND CORRECTIONS

The investigation was made in the Langley high-speed 7- by 10-foot tunnel at a Mach number of 0.186 which corresponds to a dynamic pressure of 50 pounds per square foot and at a Reynolds number per foot of 1.35×10^6. The forces and moments were measured through an angle-of-attack range from -5° to 22°. Transition strips 1/8 inch wide of No. 100 carborundum grit were placed along the wings and tail surfaces at 5 percent of the chord and around the fuselage nose at 5 percent of the fuselage length.

The angle of attack was corrected for deflection of the sting-support system under load. The drag data were corrected to correspond to a pressure at the base of the fuselage and engine nacelles equal to free-stream static pressure. A drag coefficient of 0.0016, corresponding to the theoretical internal skin-friction drag of the four nacelles, was subtracted from the data of the configuration with the nacelles on. The values of the skin-friction drag were obtained from the Kármán-Schoenherr formula presented in reference 6. Jet-boundary and blockage corrections as calculated by the methods of references 7 and 8, respectively, have been applied to the data.

PRESENTATION OF DATA

In order to aid in the location of a particular set of data, an outline of the contents of the data figures is presented as follows:

RESULTS AND DISCUSSION

The effect of modifying the nose of the fuselage can be seen from the data presented in figure 9. Over most of the angle-of-attack range, slight reductions in the lift coefficient were obtained by decreasing the length of the fuselage nose. This decrease in lift coefficient coupled with the long moment arm of the original nose produced a small improvement in the pitching-moment variation with lift coefficient. Figure 9 also indicates that the modified

fuselage nose, which as a result of the decreased nose length had less wetted area than the original nose, produced a lower value of drag coefficient and a higher maximum lift-drag ratio. The modified nose was used for the remainder of this investigation.

The effect of the outboard tails on the longitudinal aerodynamic characteristics of the configuration with wing 1 is shown in figure 10. Removing the outboard horizontal tail surfaces resulted in a decrease in the lift-curve slope and an increase in drag due to lift which are directly related to the reduction in wing area and aspect ratio of the configuration. The pitching-moment data indicate that longitudinal instability occurred at relatively low lift coefficients with the outboard tails on. Removing the outboard tails resulted in a configuration which, although unstable through zero lift coefficient, exhibited a more nearly linear pitching-moment variation with lift coefficient than did the configuration with the outboard tails on. It is evident from these data and also from the data presented in reference 4 that the pitch-up exhibited by the complete configuration is the result of a combination of a decrease in the effectiveness of the outboard tails and an increase in the effectiveness of the forward portion of the wing with increasing lift coefficient. Therefore, in an attempt to eliminate this longitudinal instability, modifications and leading-edge devices applied to both the wing and the tails have been investigated and the effects of each application will be discussed in some detail.

The effect of the addition of various flat-plate sections to the trailing edge of the basic wing (wing 1) to obtain wings 2 to 10 can be seen from the data presented in figures 11 to 14. The pitching-moment data for these wings are presented not only about a common moment center but also for ease in comparing these data, about a moment center that results in a stability level of $0.05\bar{c}$ near zero lift for each wing planform. These data indicate that the addition of area to the trailing edge of the basic wing (wing 1) resulted in a decrease in the lift-curve slope and in the minimum drag coefficient and an increase in the drag due to lift of the configuration.

For the various wing planforms, the pitching-moment data transferred to a stability level of $0.05\bar{c}$ near zero lift indicate that the addition of area to the trailing edge of the basic wing (wing 1) in the manner shown for wings 5 to 10 produced improvements in the variation of pitching-moment coefficient with lift coefficient (figs. 12 to 14). However, adding the area in the manner shown for wings 2 to 4 (fig. 11) shows only slight changes in the pitching-moment variation with lift coefficient. It is evident, therefore, that the region of the wing most effective for adding area to the trailing edge to produce improvements in the pitching-moment variation with lift coefficient is near the fuselage. Although wings 5 and 6 exhibited the most promising variation of pitching-moment coefficient with lift coefficient, wing 7 was used during most of the remainder of this investigation, because, of all the wings investigated, this wing offered the best compromise between stability and performance.

Figure 15 shows that the addition of chord extension 1 to the configuration with wing 7 resulted in an increase in the lift-curve slope, a decrease in the drag due to lift, and a slight improvement in the variation of pitching-moment coefficient with lift coefficient. This improvement in the pitching-moment

variation with lift coefficient is the result of the increased stability level through zero lift coefficient, since both pitching-moment curves, when transferred to the same stability level, are approximately the same.

The effect of cutting various sizes of slots in the forward portion of the wing (fig. 8) on the longitudinal aerodynamic characteristics of the configuration with wing 7 is presented in figure 16. These data show that definite improvements in the pitching-moment variation with lift coefficient can be obtained by having slots in the forward portion of the wing. These slots allow air to flow through the wing from the bottom surface to the top. The air flow causes a reduction in lift on this portion of the wing and a consequent improvement in the pitching-moment variation with lift coefficient. However, the pitching-moment improvement is accompanied by fairly large reductions in the maximum lift-drag ratio.

Figure 17 shows the effect of wing leading-edge flap A (fig. 5) on the longitudinal aerodynamic characteristics of the configuration with wing 7. The configuration with only the inboard section of the leading-edge flap exhibited improvements in the pitching-moment variation with lift coefficient, but the configuration with only the outboard section experienced a more severe pitch-up than that obtained without the leading-edge flaps. An investigation of the flow characteristics over the wing by use of tufts indicated that the leading-edge flap causes the flow to separate from the upper surface of the wing in the region behind the flap. This flow separation behind the leading-edge flap reduces the lift carried by the wing; inasmuch as the area of the wing affected by the inboard section of the flap is ahead of the moment center, this loss in lift improves the variation of pitching moment with lift coefficient. However, most of the area affected by the outboard section of the leading-edge flap is behind the moment center; therefore, the loss in lift caused by the flap accentuates the pitch-up characteristics of this configuration.

The data of figure 17 also indicate that the configuration with leading-edge flap A resulted in a sizable reduction in the maximum lift-drag ratio, even though the drag due to lift measured in the low lift range was slightly reduced. The lower values of drag due to lift were probably the result of the increased leading-edge radius (fig. 5) of this leading-edge flap.

A comparison of the longitudinal aerodynamic characteristics of the configuration with the two leading-edge flaps (fig. 5) on the inboard section is presented in figure 18. The use of leading-edge flap A produced a slightly better improvement in pitching moment with lift coefficient than did leading-edge flap B. Also indicated by the data is that the configuration with leading-edge flap A, owing to its larger leading-edge radius, had a lower drag due to lift and a higher maximum lift-drag ratio.

Variations in the height of leading-edge flap B above the wing surface had only a slight effect on the lift and pitching-moment characteristics of the configuration with wing 7. (See fig. 19.) However, increasing the height of the flap resulted in increases in the drag coefficient in the low lift range. This increase, in turn, reduced the maximum lift-drag ratio.

The effect of the position of the outboard tails (fig. 6) on the longitudinal aerodynamic characteristics of the configuration with wing 1 is shown in figure 20. These data show that moving the outboard tails up from position 1 to the tip of the vertical tails (position 2) resulted in no appreciable change in the aerodynamic characteristics. However, moving the tails inboard of the vertical tails (position 3) resulted in a configuration which, in the lift-coefficient range below 0.3, showed only slightly less instability than that obtained with the outboard horizontal tails removed (fig. 10). At higher lift coefficients the stability increased and then decreased so that at lift coefficients above 0.70 the instability was greater than that at zero lift. In contrast, the outboard tail configurations (positions 1 and 2) showed instability at all lift coefficients above 0.35. The data of reference 4 show that the outboard tails in the original position (position 1) are in a region of increasing upwash angles at low angles of attack. At the higher angles of attack these data indicate that the outboard tails are losing effectiveness; this loss can be caused by the tails moving out of the region of increasing upwash angles or by tail stall. Both these causes will result in a loss in lift on the tails and in an accompanying reduction in longitudinal stability. In the case presented herein the loss in lift on the outboard tails and in the associated pitch-up is believed to be the result of a combination of the two characteristics, since methods to reduce tail stall, as will be discussed subsequently, resulted in only slight changes in the pitching-moment variation with lift. Studies of this configuration indicated that the tails in position 3 are probably in a downwash field at low angles of attack and would cause, therefore, the large stability reduction at low lift coefficients. At higher angles of attack the position of the vortex is such that the tails move into a region of increasing upwash angles. These upwash angles appear to increase rapidly and result in the increased stability in the lift-coefficient range between 0.40 and 0.70. However, above a lift coefficient of 0.70, the position of the vortex probably reduces the upwash angles of the tails. This reduction results in a loss in lift and in the accompanying pitch-up. The data of figure 20 also indicate that moving the tails from position 1 to position 3 decreases the maximum lift-drag ratio from 8.7 to 7.9. This loss is to be expected since the effective aspect ratio of the configuration is reduced.

The effect of replacing the original outboard tails with T-tails, having the same total planform area, on the longitudinal aerodynamic characteristics of the configuration with wing 1 is shown in figure 21 which indicates that the replacement resulted in a slight increase in the lift coefficient at which longitudinal instability occurs. A small reduction in lift and in maximum lift-drag ratio also resulted from the use of the T-tails.

The previously mentioned tuft studies that were made on this configuration indicated the possibility of separation along the leading edge of the outboard tails. This separation can probably be expected, for the outboard tails have an airfoil section that has a sharp leading edge. In an attempt to eliminate this leading-edge separation, chord extension 2 was placed on the outboard tails. As indicated by the data presented in figure 23, chord extension 2 was at least partially effective in reducing the leading-edge separation. That is, the addition of chord extension 2 to either the configuration with leading-edge flap A

or the configuration without leading-edge flap A resulted in slight improvements in the pitching-moment variation with lift coefficient at the higher lift coefficients.

As a partial summary of the combined effect of several of the modifications studied during the present investigation, figure 24 was prepared. The data of this figure show a comparison of the aerodynamic characteristics of the original configuration without the nacelles, as shown in reference 4, with the configuration incorporating several of the modifications studied during the present investigation. These data show that, although linear variations of pitching moment with lift coefficient were not obtained by the use of these modifications, considerable improvements are evident and that further tailoring of these modifications could possibly give a linear pitching-moment variation with lift coefficient. This comparison also indicates that losses in the lift coefficient at a given angle of attack and in the maximum lift-drag ratio accompanied these improvements in the pitching-moment variation with lift coefficient. The effect shown in figure 22 of the engine nacelles, however, implies that the lack of engine nacelles on the configuration with wing 1 accounts for most of the increase in maximum lift-drag ratio. (See fig. 24.)

CONCLUSIONS

An investigation was conducted to determine the effects of wing and outboard-tail modifications on the longitudinal aerodynamic characteristics of a highly swept, blended wing-body, supersonic commercial air transport (SCAT) configuration. The modifications examined in this investigation included wing trailing-edge planform changes, leading-edge chord extensions, wing upper-surface leading-edge flaps, wing-body juncture slots, and various arrangements of the outboard tail surfaces. The investigation made at a Mach number of 0.186, at a test Reynolds number per foot of 1.35×10^6, and at angles of attack from -5° to 22° indicates the following conclusions:

1. Modifications and leading-edge devices applied individually to the wing or outboard tail surfaces of this configuration generally produced small improvements in the pitching-moment variation with lift coefficient.

2. When combinations of these modifications and leading-edge devices were employed, nearly linear variations of pitching-moment coefficient with lift coefficient were obtained.

3. Applying these modifications and leading-edge devices to the configuration usually resulted in reductions in the lift coefficient at a given angle of attack and in the maximum lift-drag ratio.

Langley Research Center,
National Aeronautics and Space Administration,
Langley Station, Hampton, Va., December 7, 1964.

REFERENCES

1. Spearman, M. Leroy; Driver, Cornelius; and Robins, A. Warner: Aerodynamic Characteristics at Mach Numbers of 2.30, 2.96, and 3.50 of a Supersonic Transport Model With a Blended Wing-Body, Variable-Sweep Auxiliary Wing Panels, and Outboard Tail Surfaces. NASA TM X-803, 1963.

2. Alford, William J., Jr.; Hammond, Alexander D.; and Henderson, William P.: Low-Speed Stability Characteristics of a Supersonic Transport Model With a Blended Wing-Body, Variable-Sweep Auxiliary Wing Panels, Outboard Tail Surfaces, and Simplified High-Lift Devices. NASA TM X-802, 1963.

3. Robins, A. Warner; Spearman, M. Leroy; and Harris, Roy V., Jr.: Aerodynamic Characteristics at Mach Numbers of 2.30, 2.60, and 2.96 of a Supersonic Transport Model With a Blended Wing-Body, Variable-Sweep Auxiliary Wing Panels, Outboard Tail Surfaces, and a Design Mach Number of 2.6. NASA TM X-815, 1963.

4. Henderson, William P.: Low-Speed Aerodynamic Characteristics of a Supersonic Transport Model With a Blended Wing-Body, Variable-Sweep Auxiliary Wing Panels, and Outboard Tail Surfaces. NASA TM X-993, 1964.

5. Anon.: Proceedings of NASA Conference on Supersonic-Transport Feasibility Studies and Supporting Research - September 17-19, 1963. NASA TM X-905, 1963.

6. Peterson, John B.: A Comparison of Experimental and Theoretical Results for the Compressible Turbulent-Boundary-Layer Skin Friction With Zero Pressure Gradient. NASA TN D-1795, 1963.

7. Gillis, Clarence L.; Polhamus, Edward C.; and Gray, Joseph L., Jr.: Charts for Determining Jet-Boundary Corrections for Complete Models in 7- by 10-Foot Closed Rectangular Wind Tunnels. NACA WR L-123, 1945. (Formerly NACA ARR L5G31.)

8. Herriot, John G.: Blockage Corrections for Three-Dimensional-Flow Closed-Throat Wind Tunnels, With Consideration of the Effect of Compressibility. NACA Rept. 995, 1950. (Supersedes NACA RM A7B28.)

TABLE I.- REFERENCE DIMENSIONS FOR WINGS

Wing	S, sq ft	$\bar{c}$, in.
1	6.096	31.333
2	6.851	36.378
3	7.004	36.844
4	7.292	37.437
5	7.789	41.981
6	8.312	45.347
7	6.903	38.181
8	7.100	39.781
9	7.339	42.422
10	7.429	42.636

TABLE II.- TRAILING-EDGE ORDINATES FOR SEVERAL WINGS

Wing 1 (basic wing)	
$\frac{y}{b/2}$	$\frac{x}{b/2}$
0	0.750
.125	.912
.188	.975
.250	.981
.312	.952
.375	.895
.625	.525
.975	0

Wing 2	
$\frac{y}{b/2}$	$\frac{x}{b/2}$
0	0.750
.103	.750
.125	.749
.188	.738
.250	.719
.313	.679
.375	.628
.500	.531
.625	.431
.756	.329

Wing 3	
$\frac{y}{b/2}$	$\frac{x}{b/2}$
0	0.750
.103	.750
.125	.744
.188	.725
.250	.688
.313	.634
.375	.576
.500	.462
.625	.346
.750	.231
.875	.113
.938	.056

Wing 4	
$\frac{y}{b/2}$	$\frac{x}{b/2}$
0	0.750
.103	.750
.125	.741
.188	.706
.250	.647
.313	.578
.375	.513
.500	.381
.625	.247
.750	.114
.875	-.019
.947	-.100

Wing 7	
$\frac{y}{b/2}$	$\frac{x}{b/2}$
0	0.563
.103	.563
.125	.586
.188	.630
.250	.655
.313	.671
.375	.670
.438	.658
.500	.632
.601	.563

Wing 8	
$\frac{y}{b/2}$	$\frac{x}{b/2}$
0	0.375
.103	.375
.125	.421
.188	.512
.250	.568
.313	.594
.375	.600
.438	.591
.500	.569
.563	.530
.625	.480
.725	.378

Wing 9	
$\frac{y}{b/2}$	$\frac{x}{b/2}$
0	0.188
.103	.188
.125	.266
.188	.404
.250	.479
.313	.522
.375	.531
.438	.522
.500	.499
.563	.463
.625	.416
.688	.364
.750	.305
.850	.193

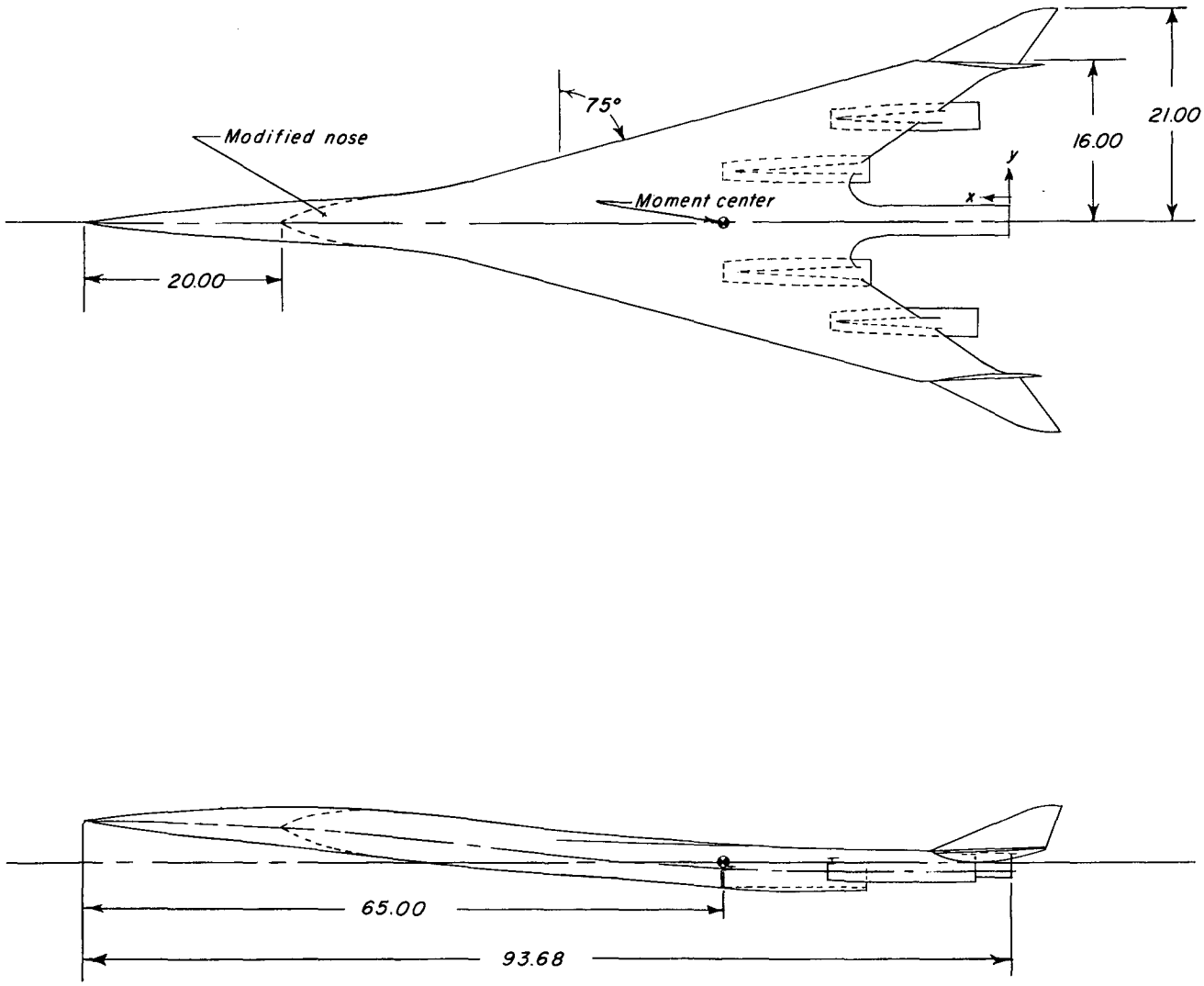

Figure 1.- Basic configuration (wing 1). All dimensions are in inches unless otherwise noted.

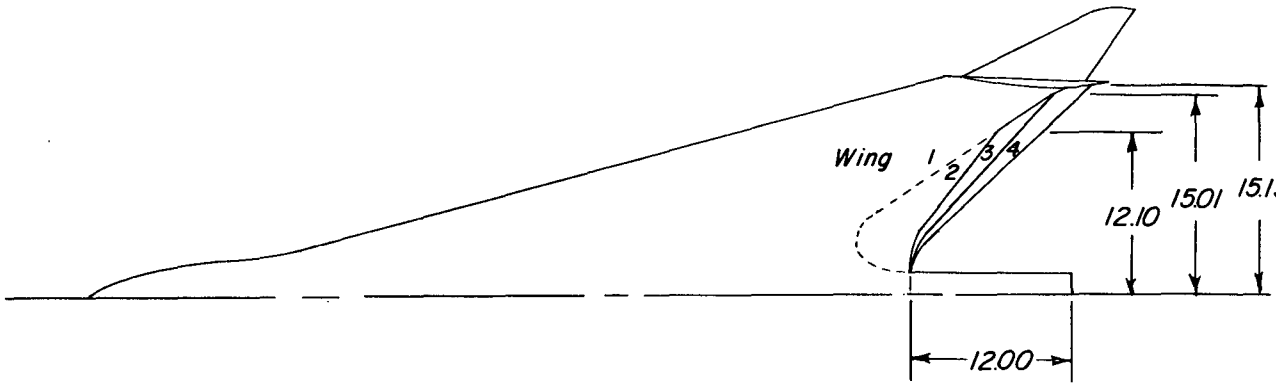

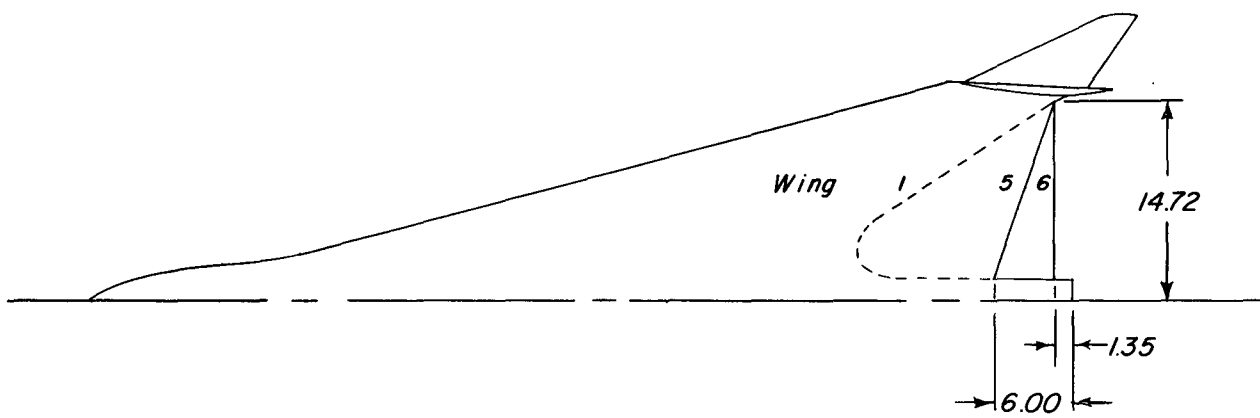

Figure 2.- Wing planforms 1 to 6. All dimensions are in inches.

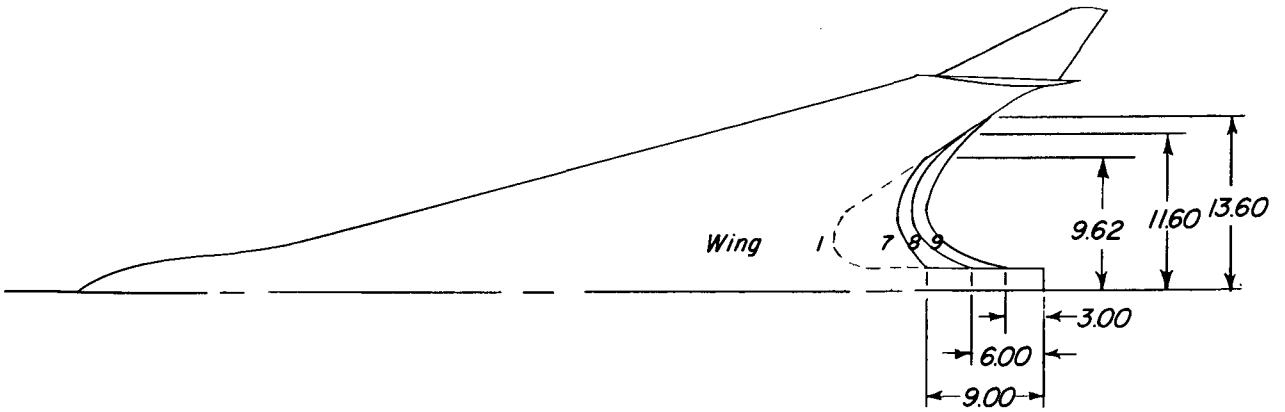

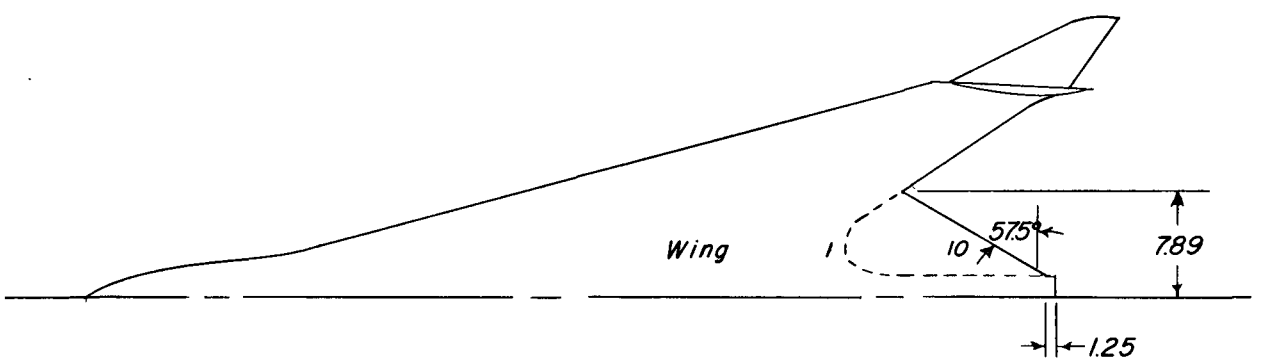

Figure 3.- Wing planforms 1 and 7 to 10. All dimensions are in inches unless otherwise noted.

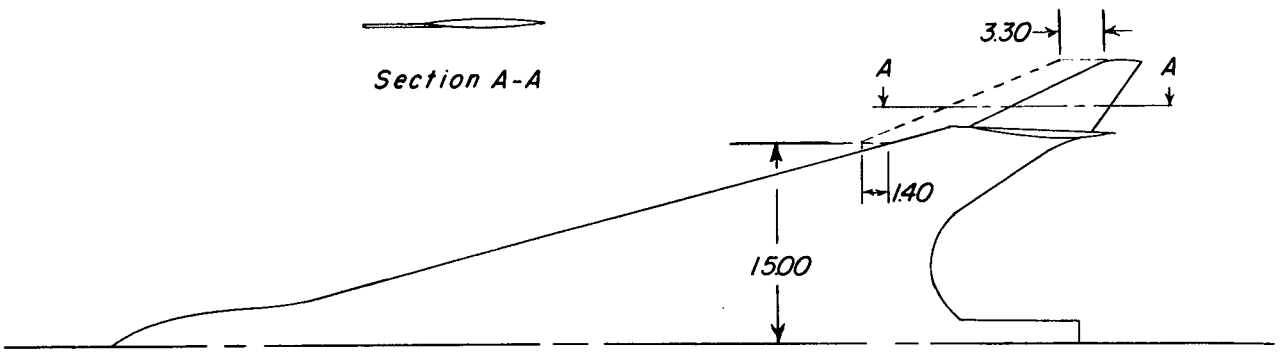

(a) Chord extension 1.

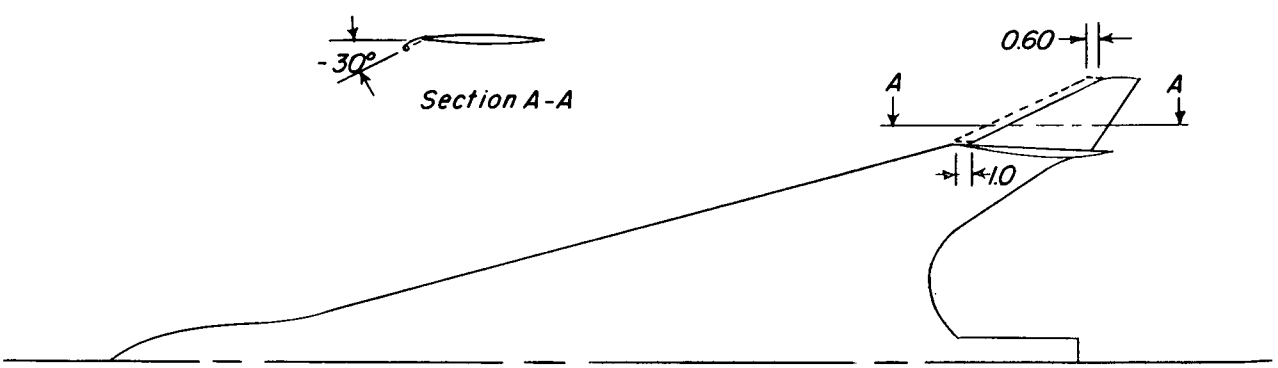

(b) Chord extension 2.

Figure 4.- Chord extensions on configuration with wing 7. All dimensions are in inches unless otherwise noted.

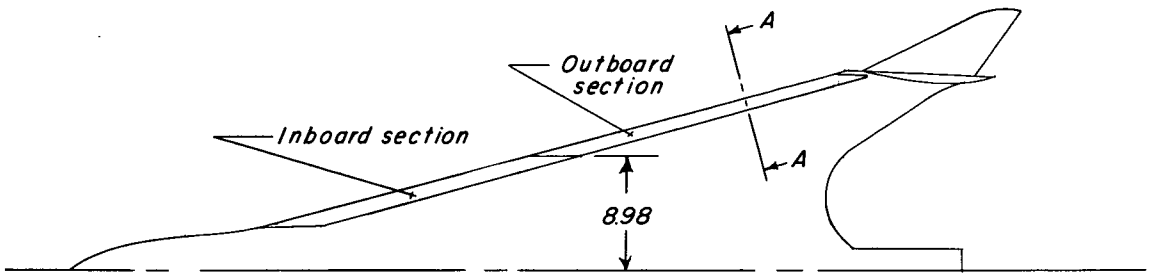

Enlarged drawing of section A-A

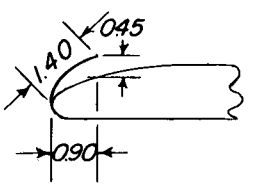

Leading edge flap A

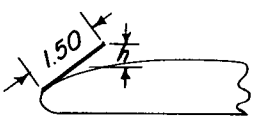

Leading edge flap B

h=0.25, 0.45 and 0.80

Figure 5.- Wing leading-edge flaps on configuration with wing 7.
All dimensions are in inches.

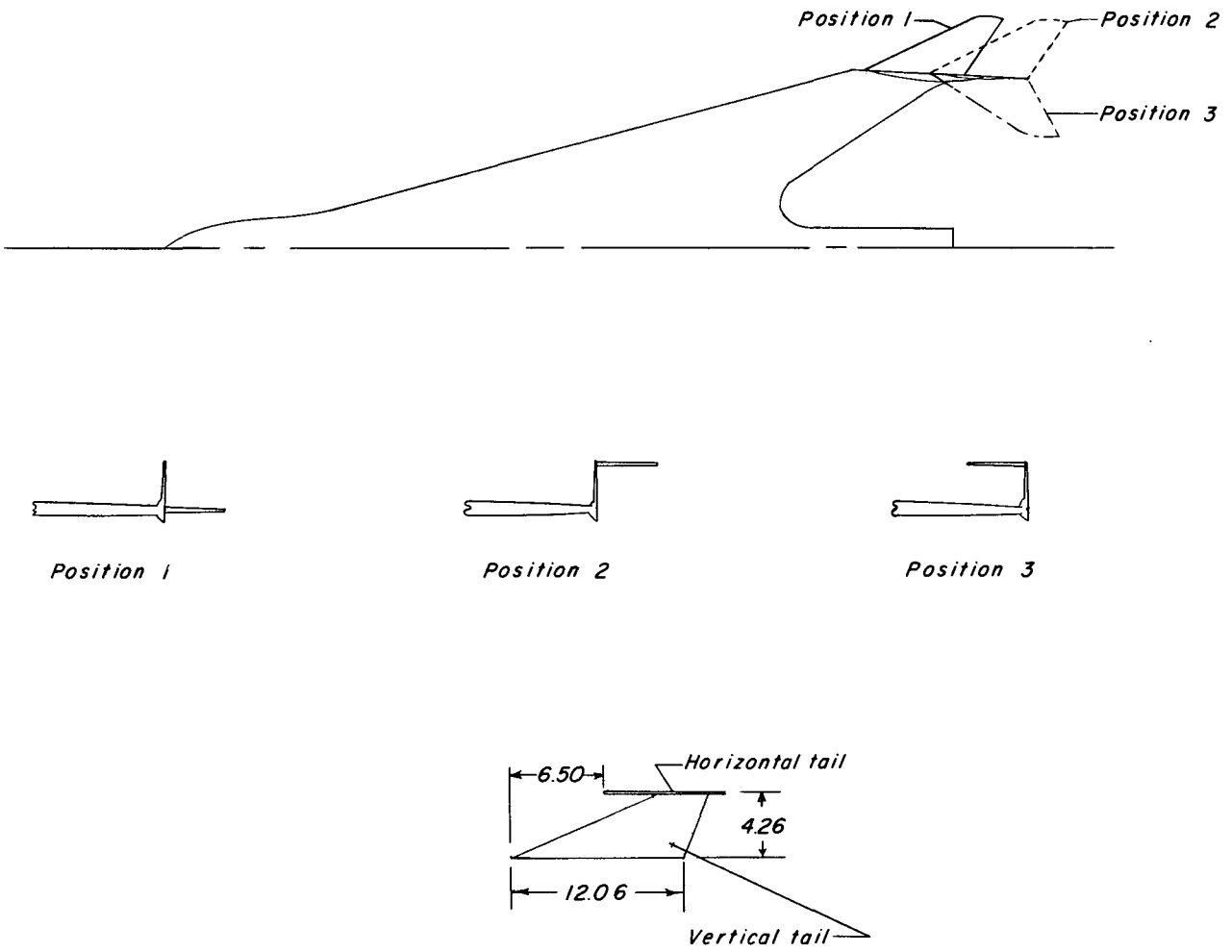

Figure 6.- Various positions of original outboard tails mounted on configuration with wing 7. All dimensions are in inches.

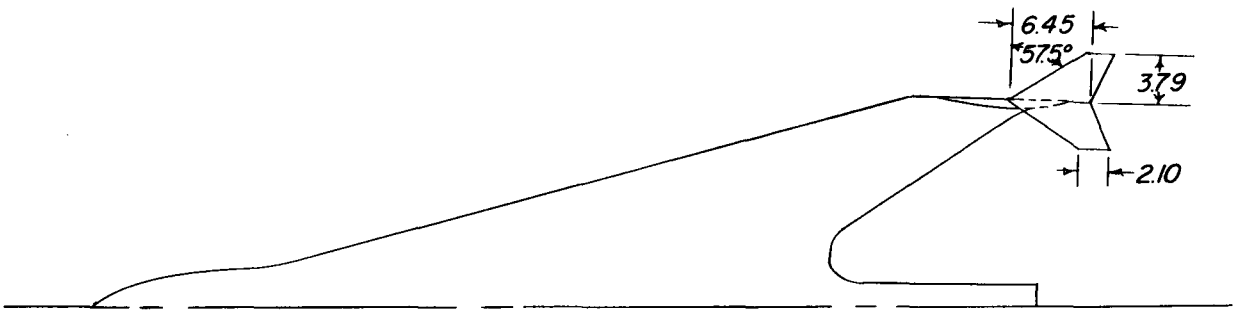

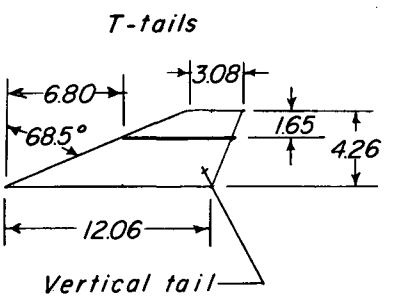

Figure 7.- T-tails mounted on configuration with wing 1. All dimensions are in inches unless otherwise noted.

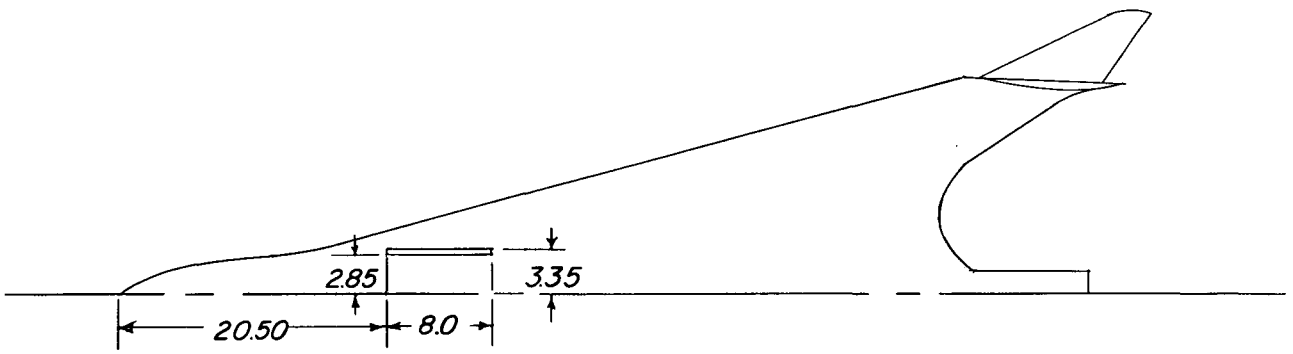

Slot configuration A

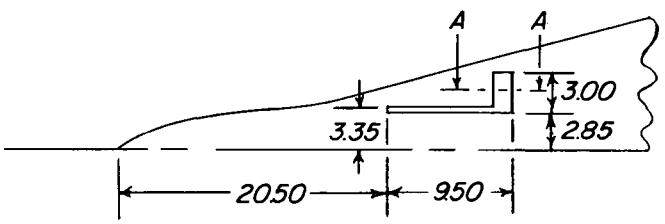

Slot configuration B

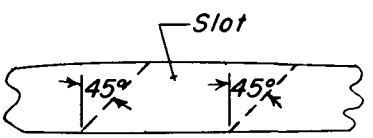

Enlarged drawing of section A-A

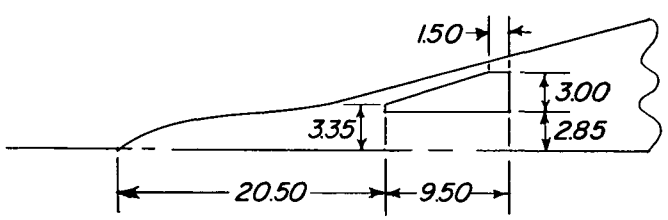

Slot configuration C

Figure 8.- Wing slots on configuration with wing 7. All dimensions are in inches unless otherwise noted.

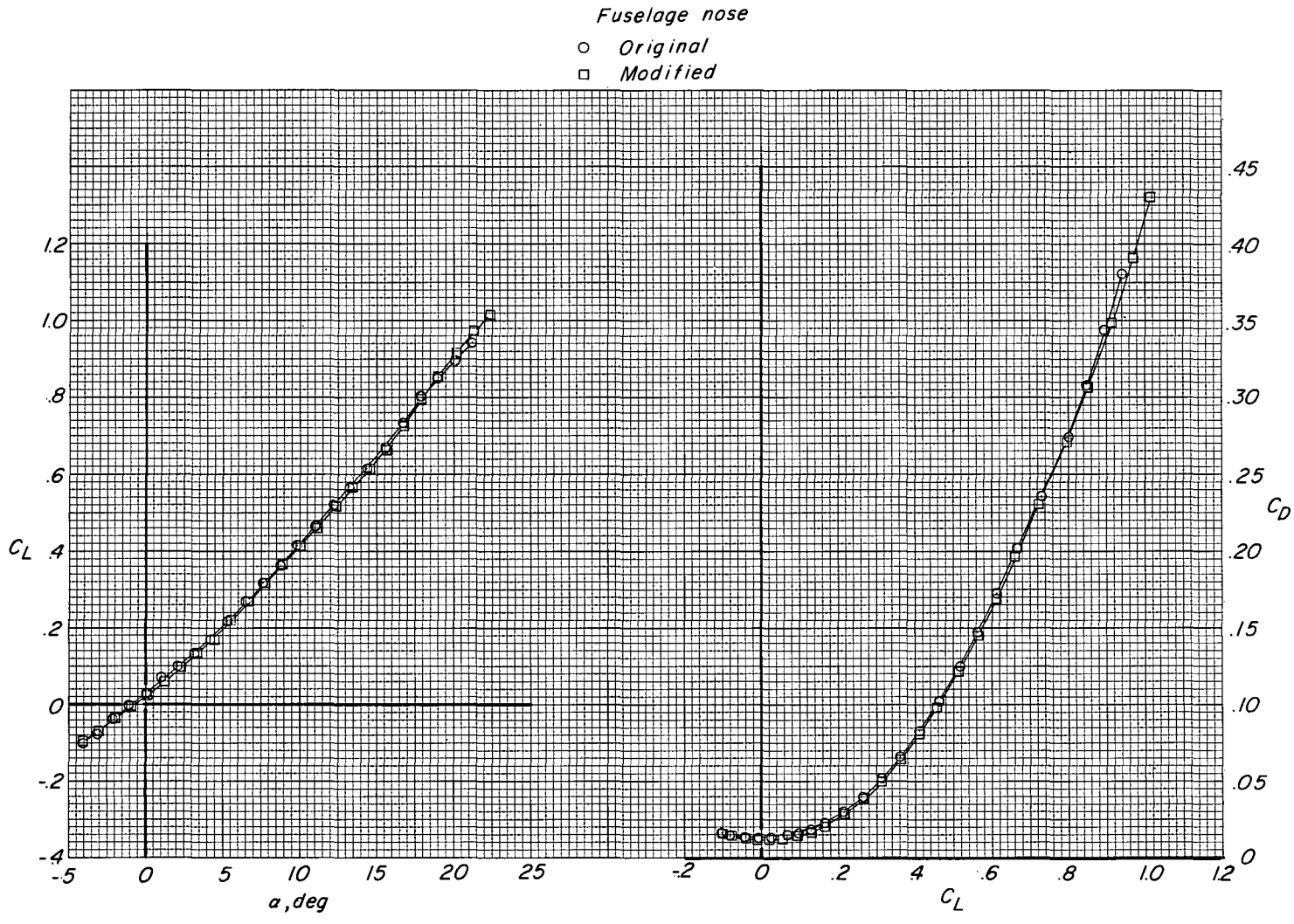

Figure 9.- Effect of fuselage nose modification on longitudinal aerodynamic characteristics of configuration with wing 1. Engine nacelles off.

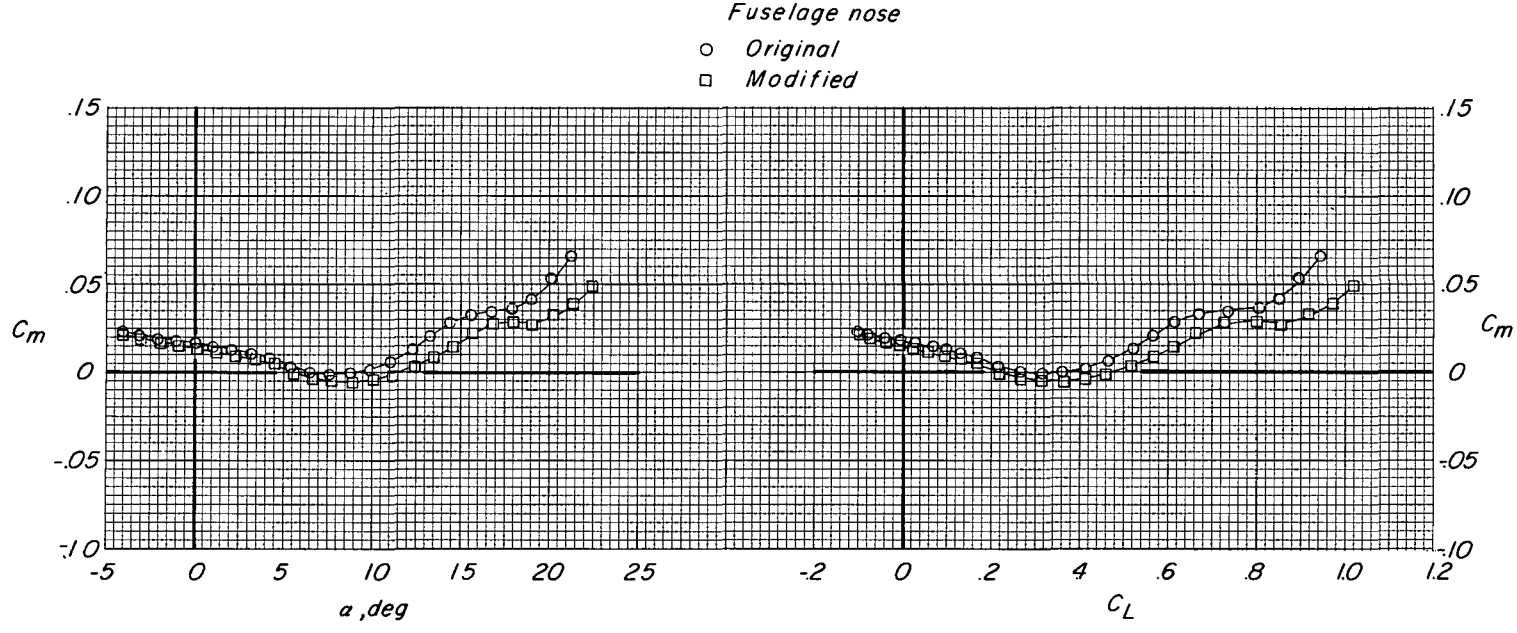

Figure 9.- Continued.

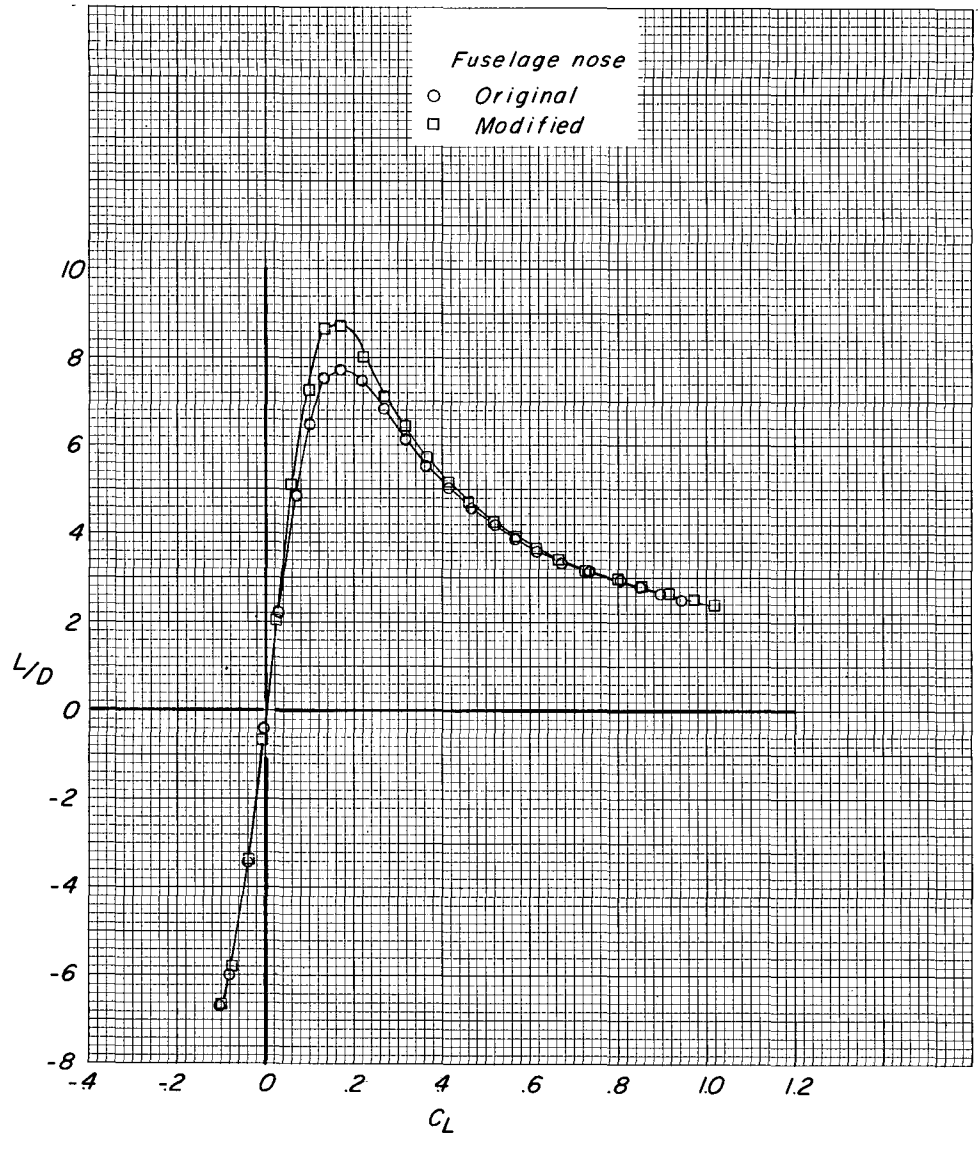

Figure 9.- Concluded.

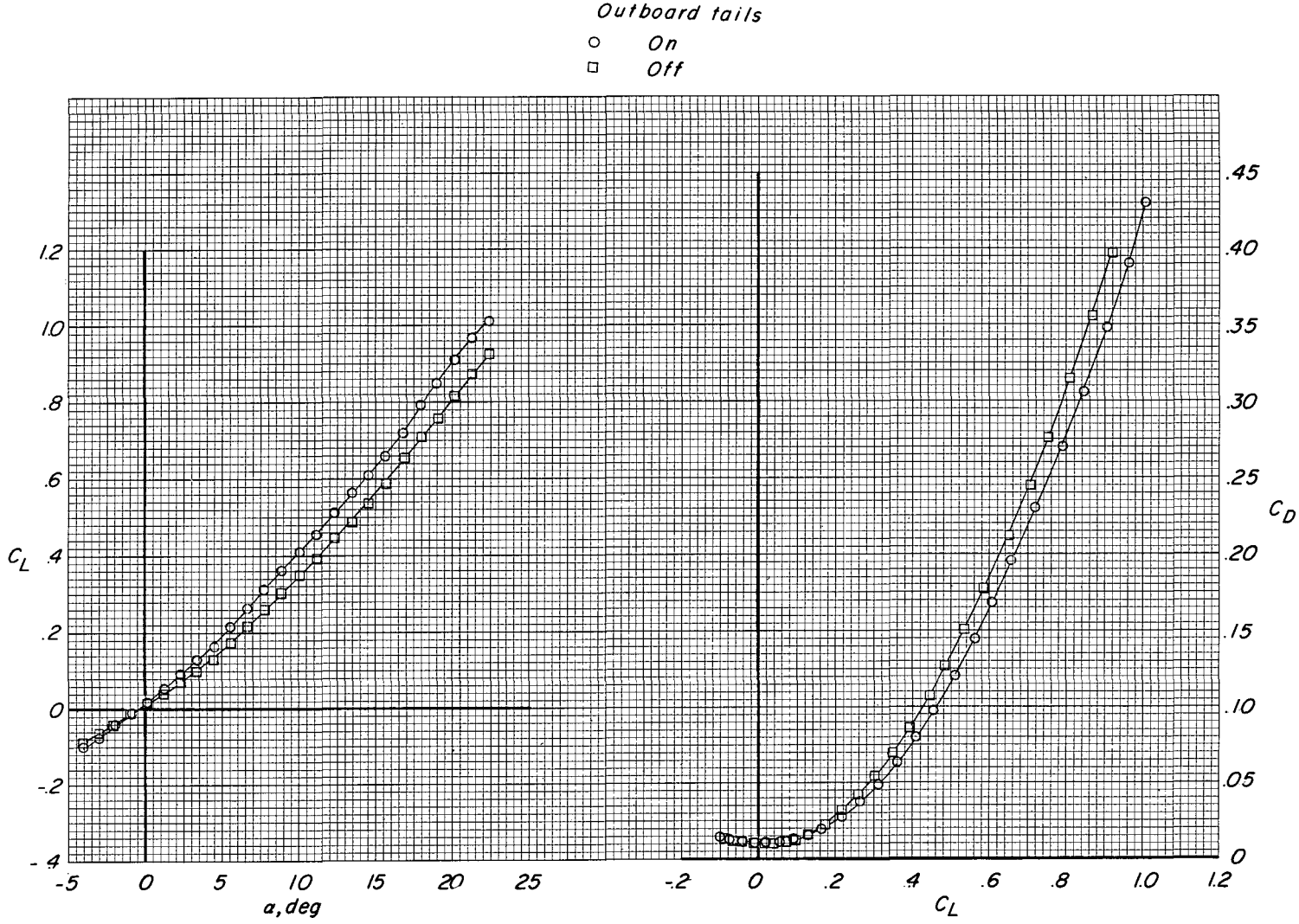

Figure 10.- Effect of outboard tails on longitudinal aerodynamic characteristics of configuration with modified fuselage nose and wing 1. Engine nacelles off.

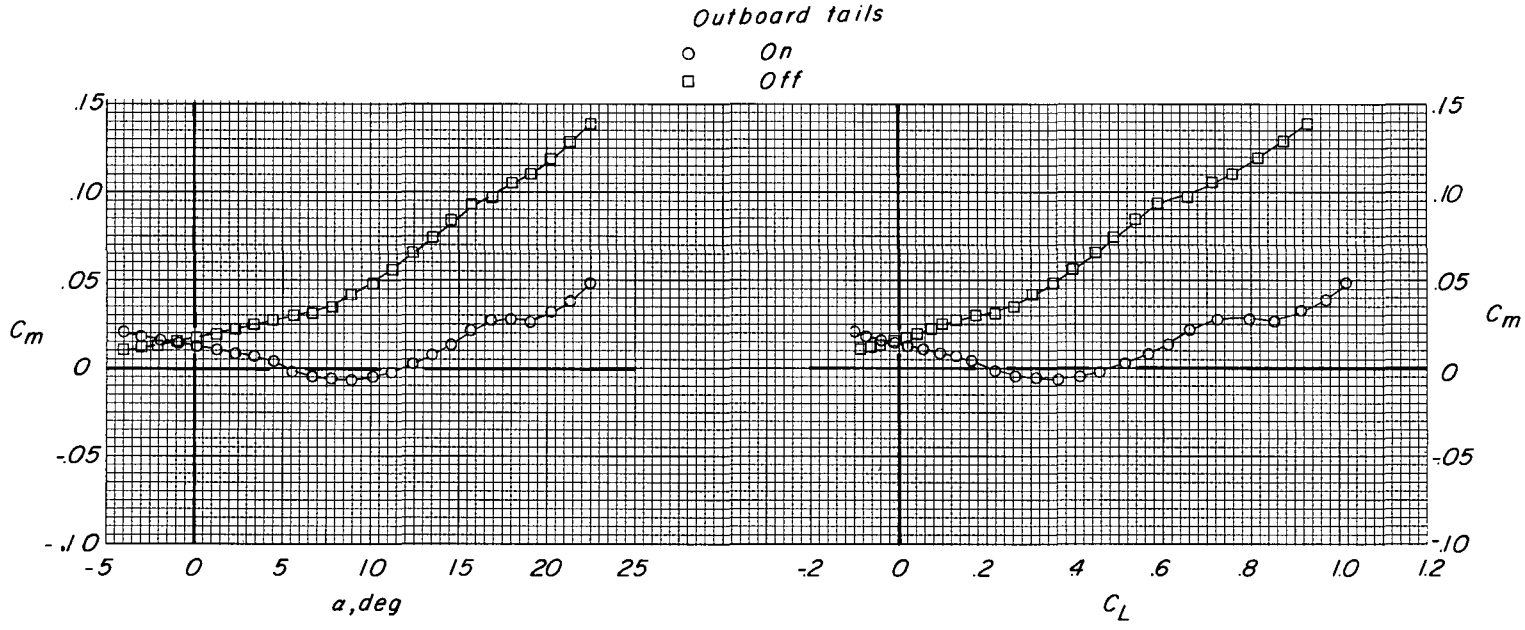

Figure 10.- Continued.

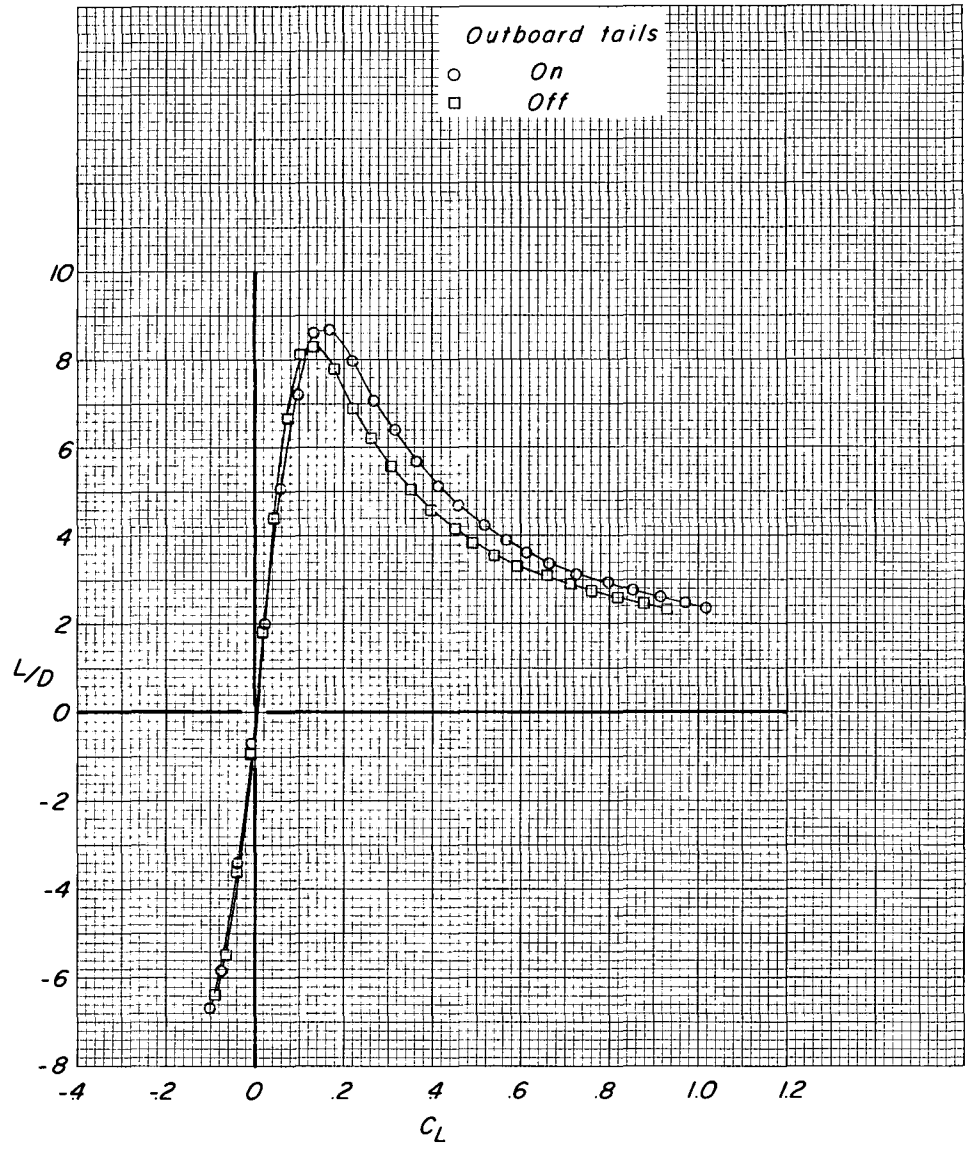

Figure 10.- Concluded.

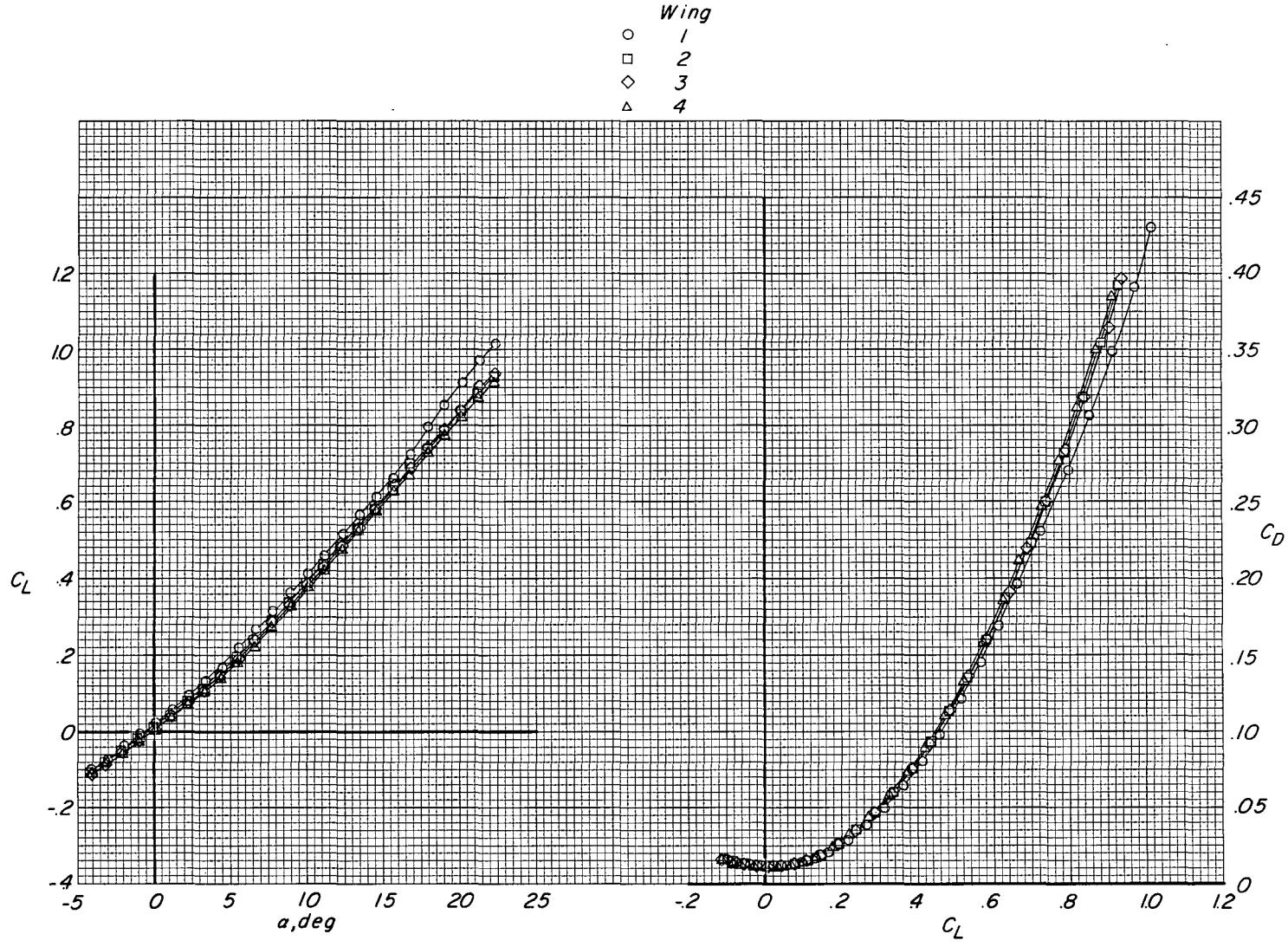

Figure 11.- Effect of wing planform on longitudinal aerodynamic characteristics of configurations with modified fuselage nose. Engine nacelles off; wings 1 to 4.

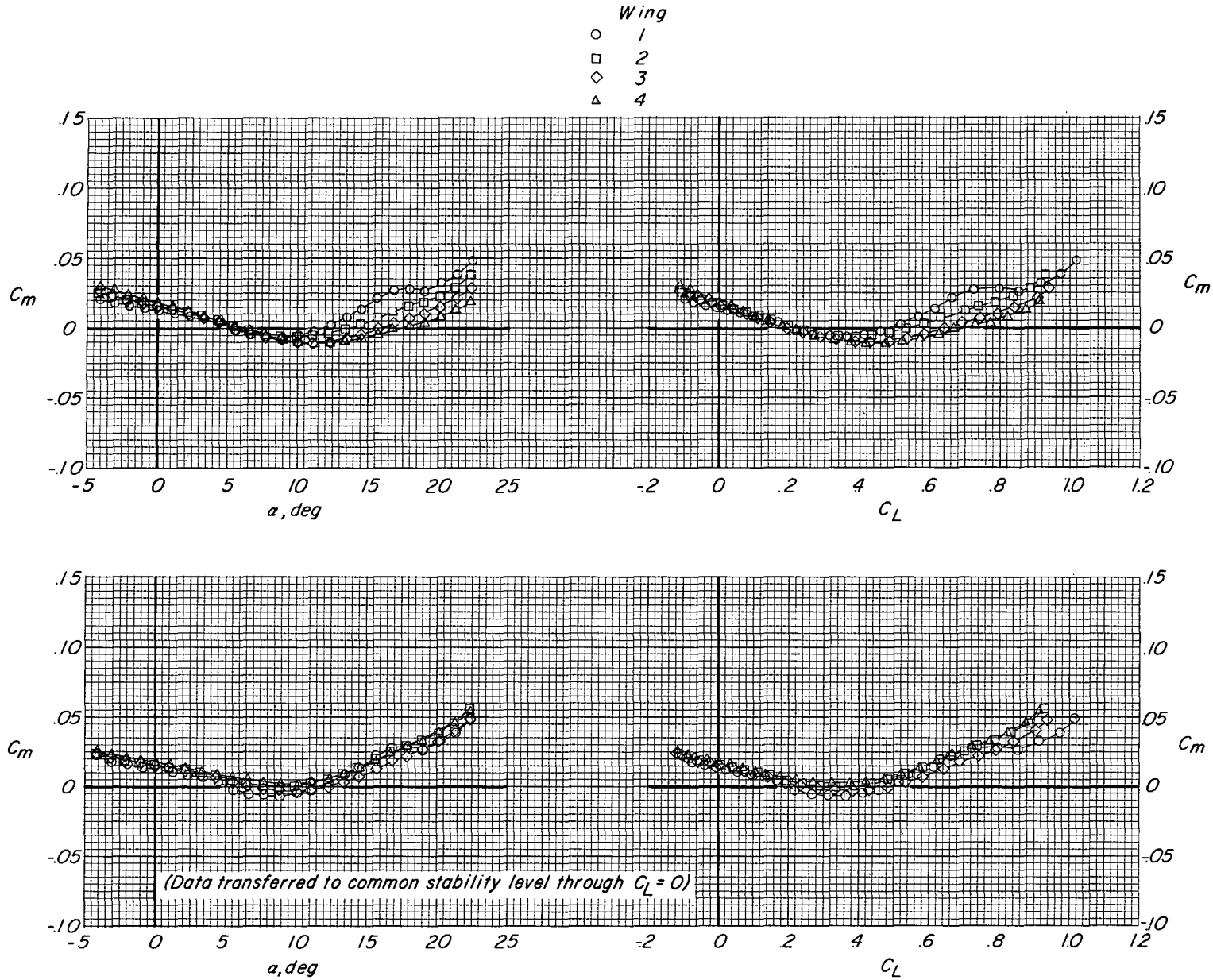

Figure 11.- Continued.

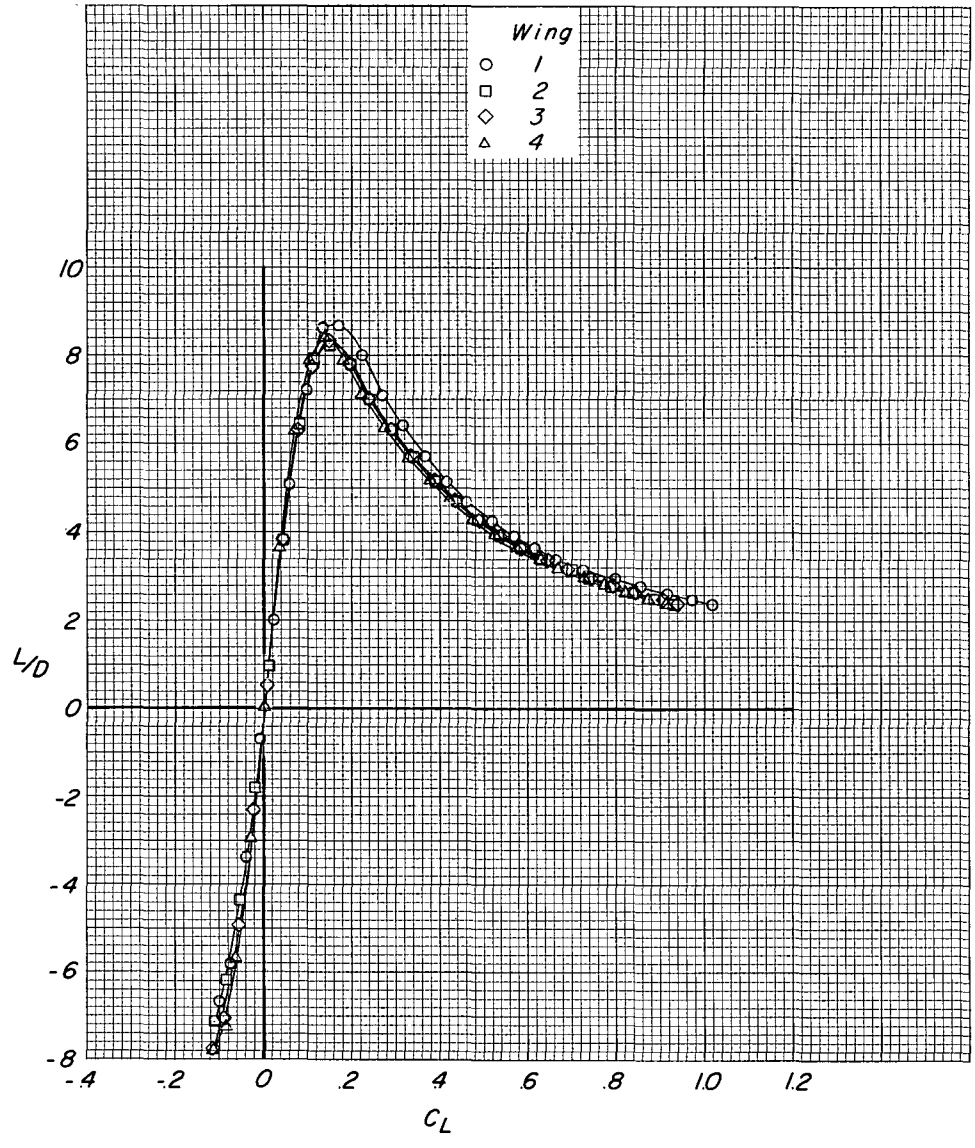

Figure 11.- Concluded.

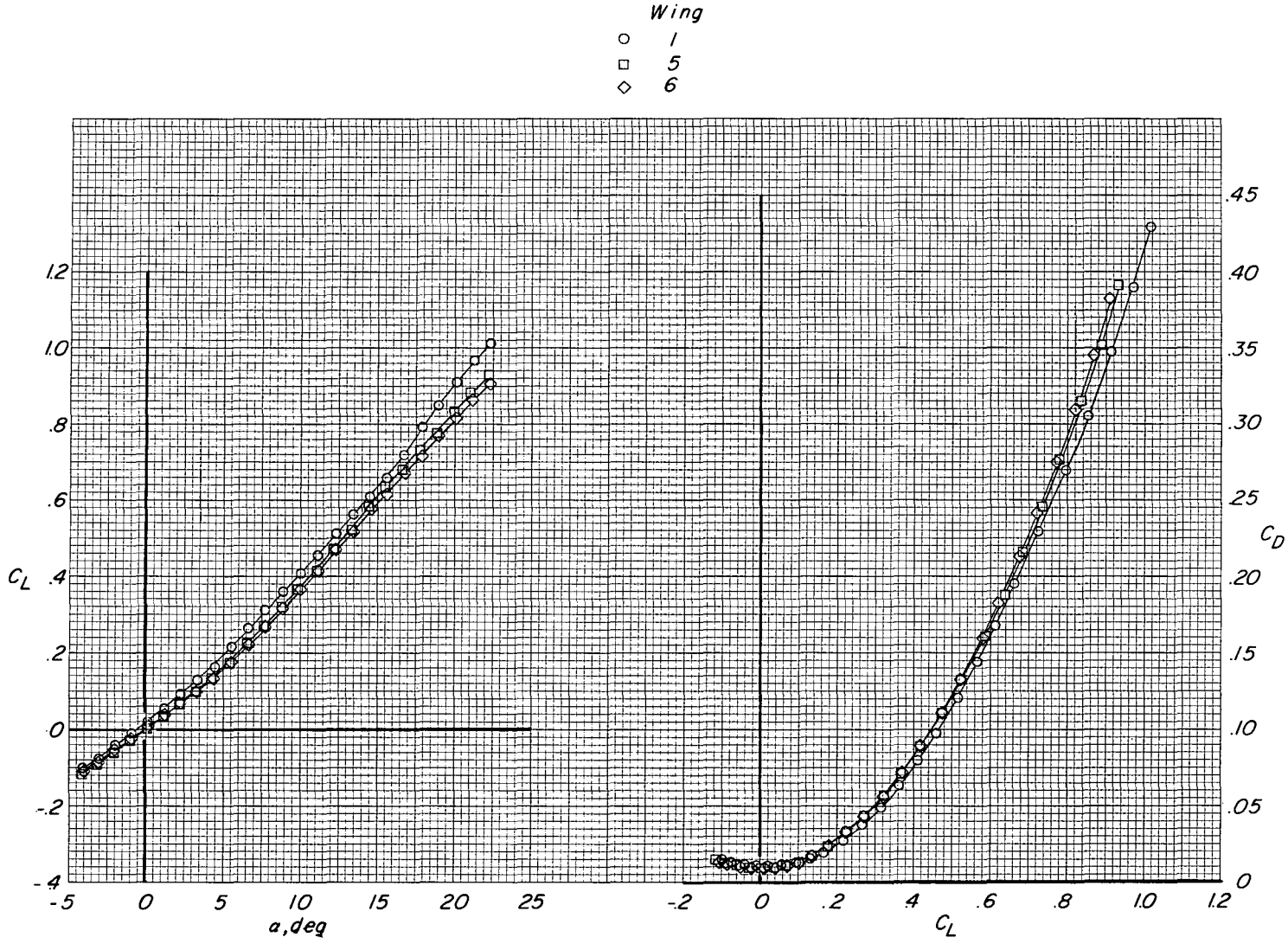

Figure 12.- Effect of wing planform on longitudinal aerodynamic characteristics of configurations with modified fuselage nose. Engine nacelles off; wings 1, 5, and 6.

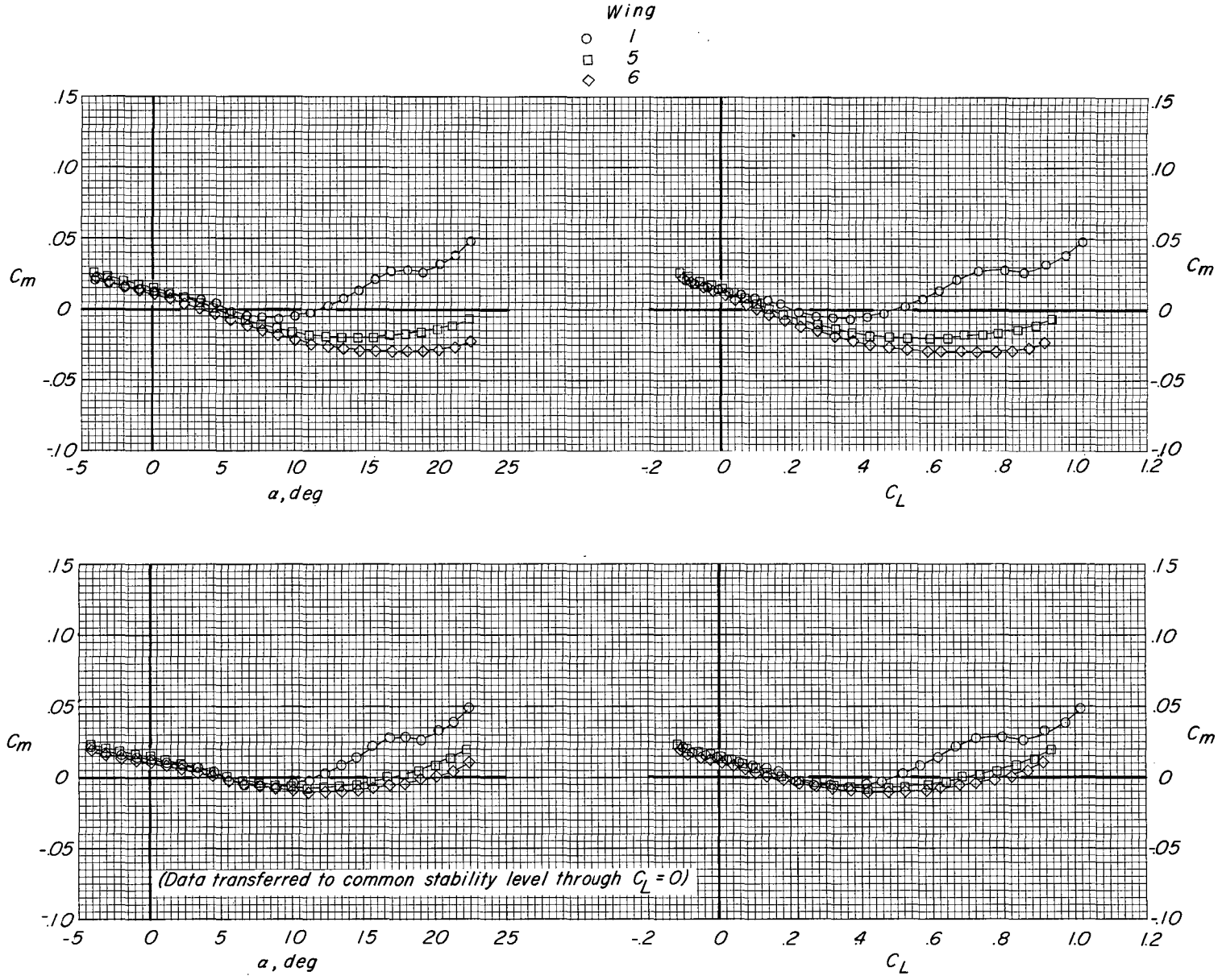

Figure 12.- Continued.

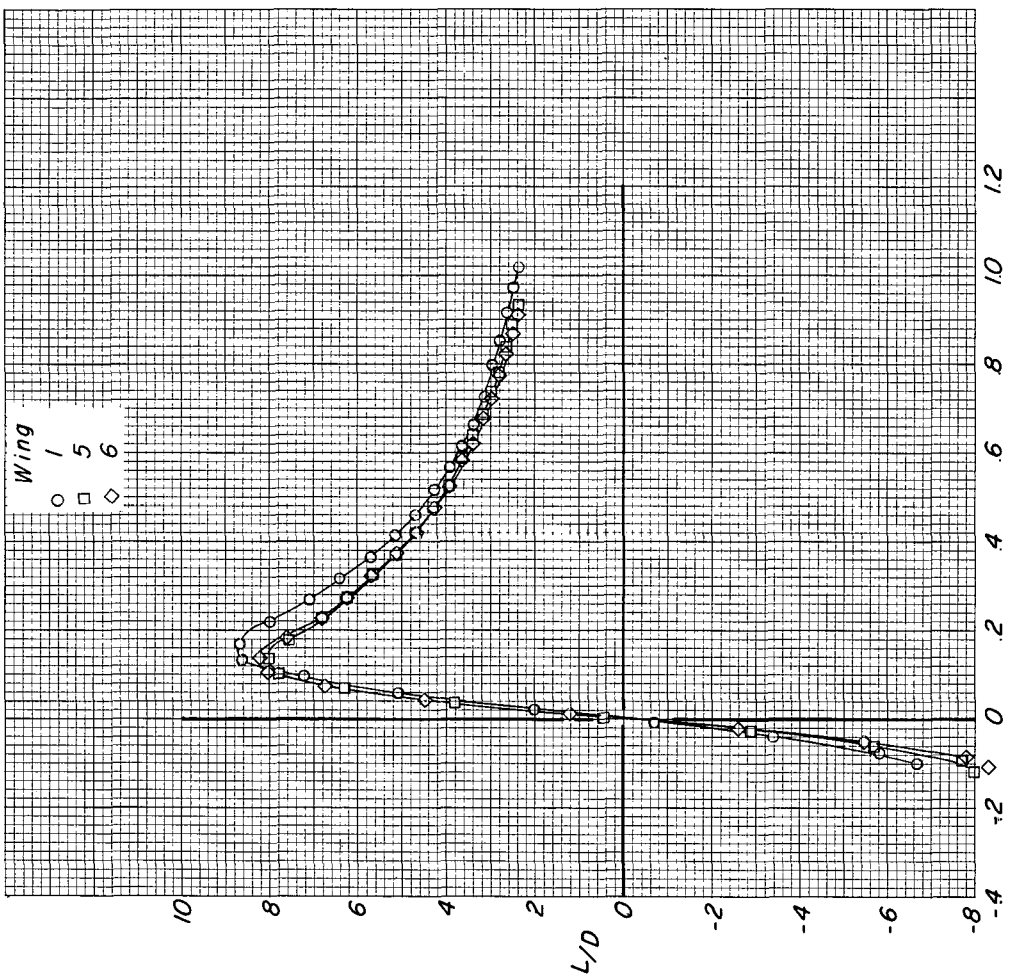

Figure 12.- Concluded.

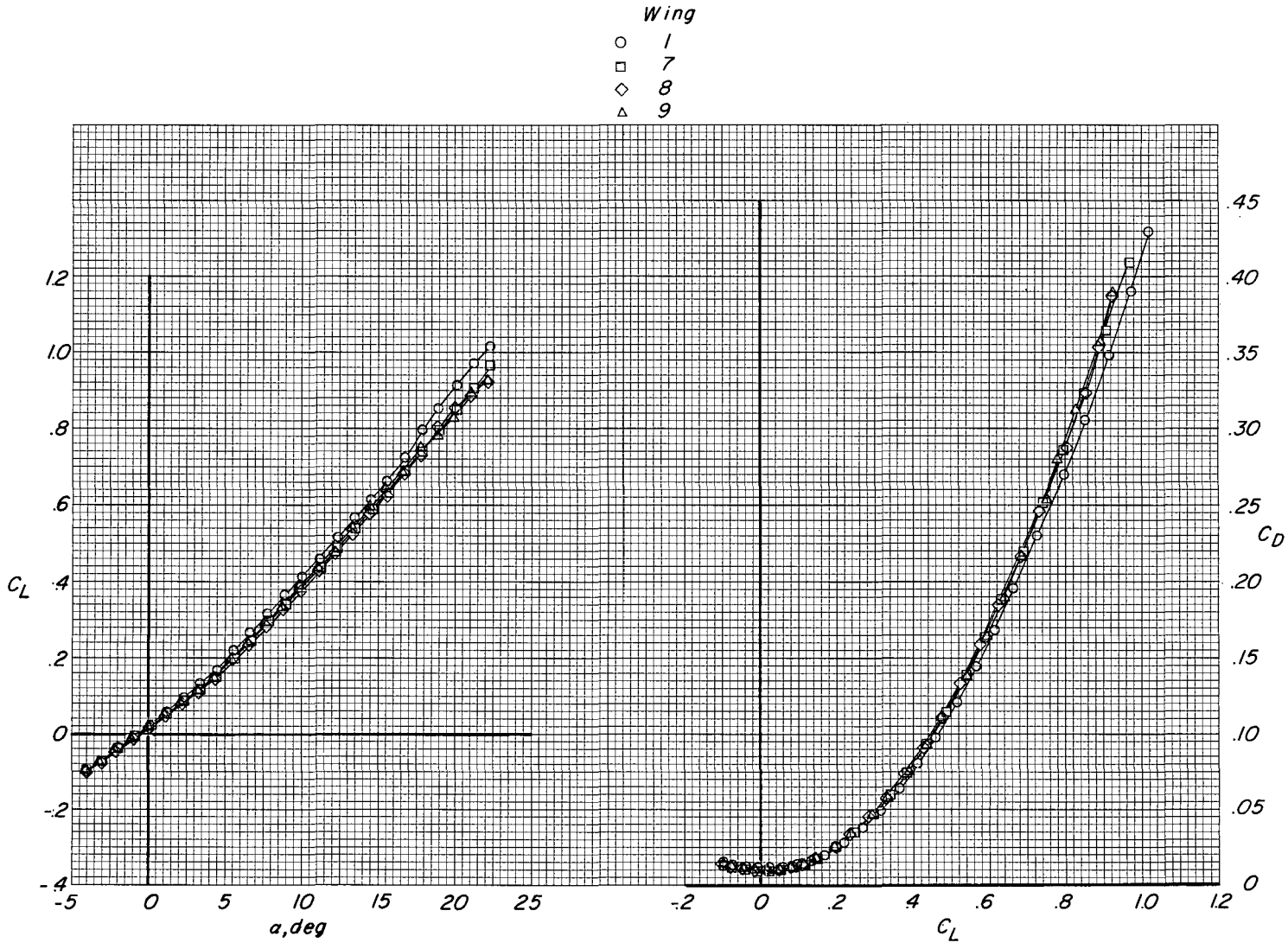

Figure 13.- Effect of wing planform on longitudinal aerodynamic characteristics of configurations with modified fuselage nose. Engine nacelles off; wings 1 and 7 to 9.

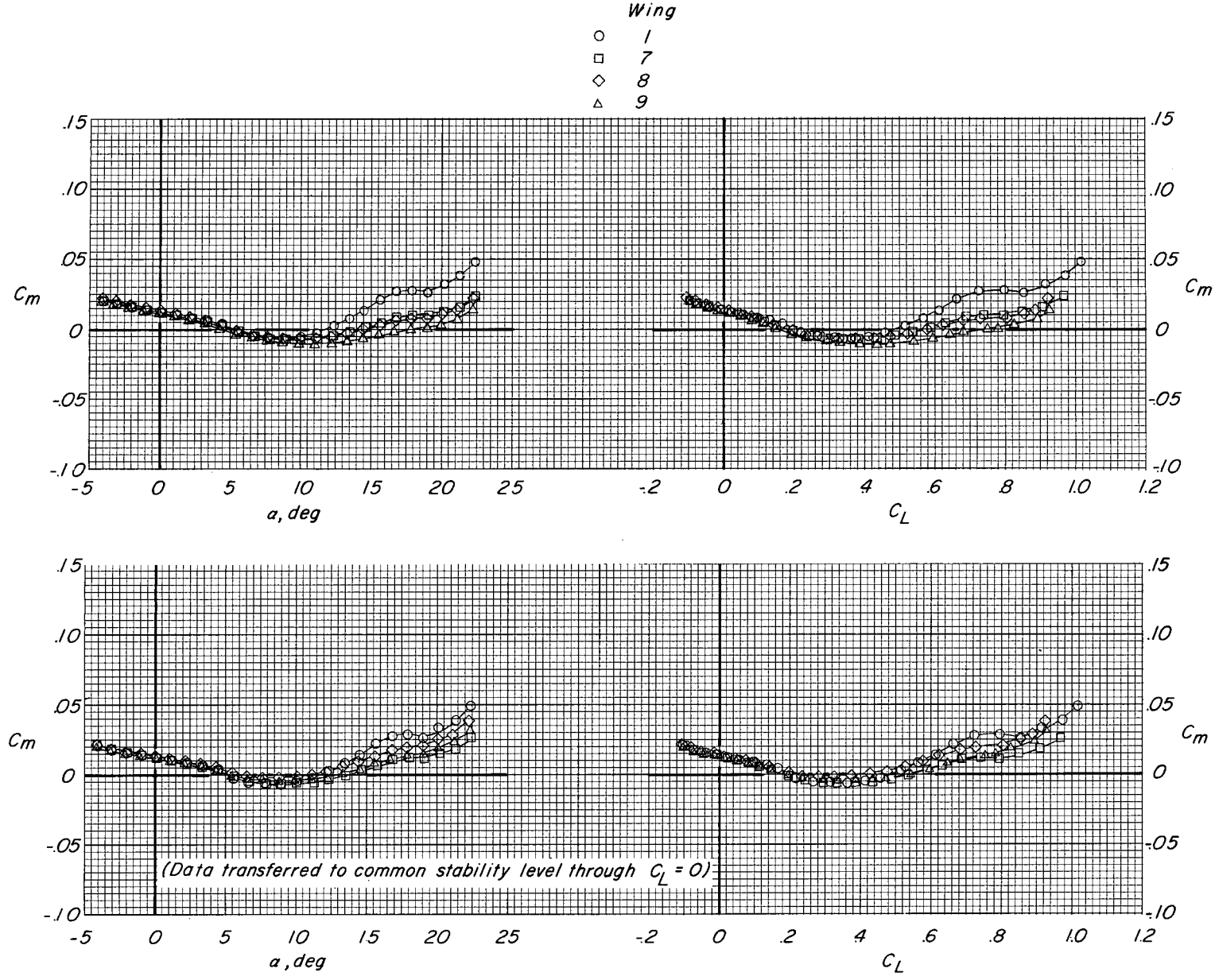

Figure 13.- Continued.

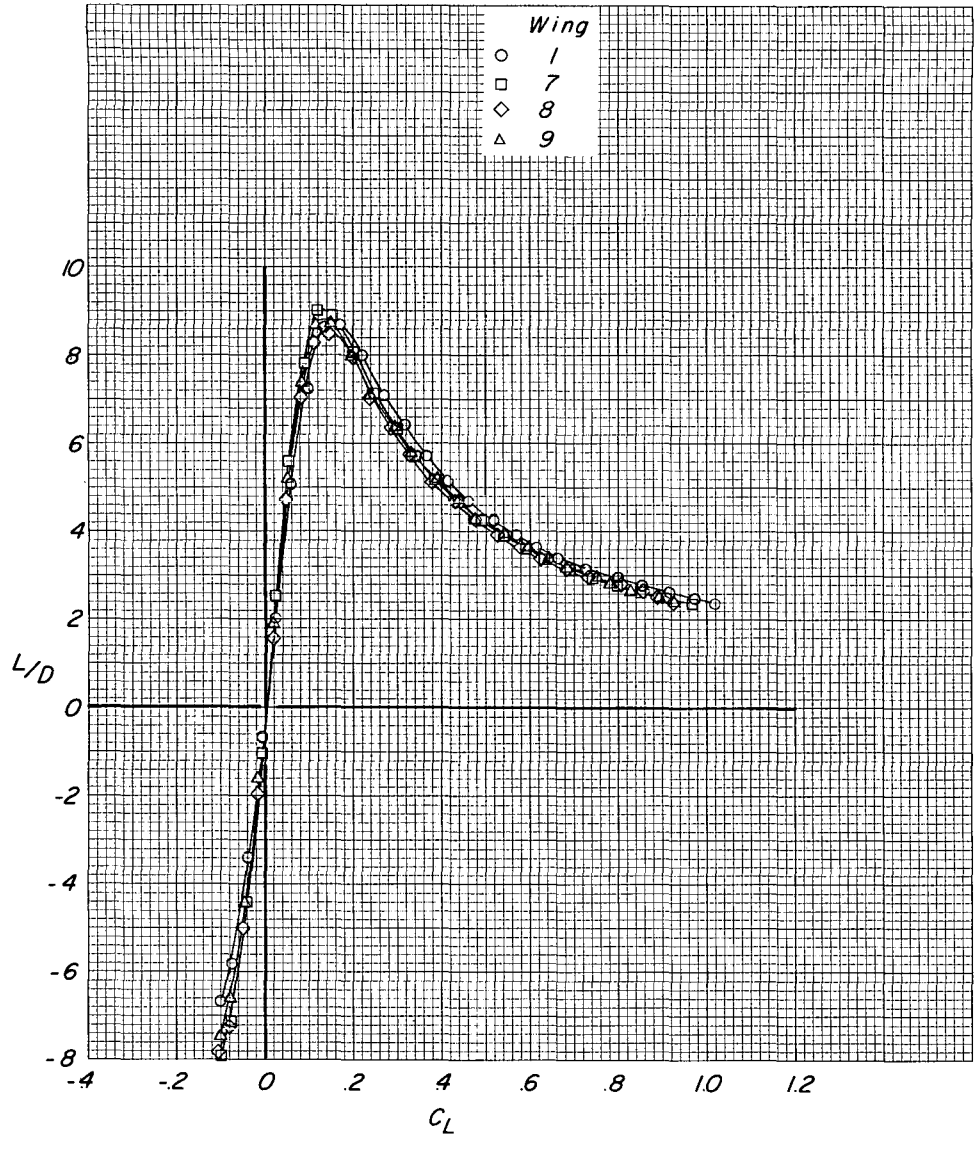

Figure 13.- Concluded.

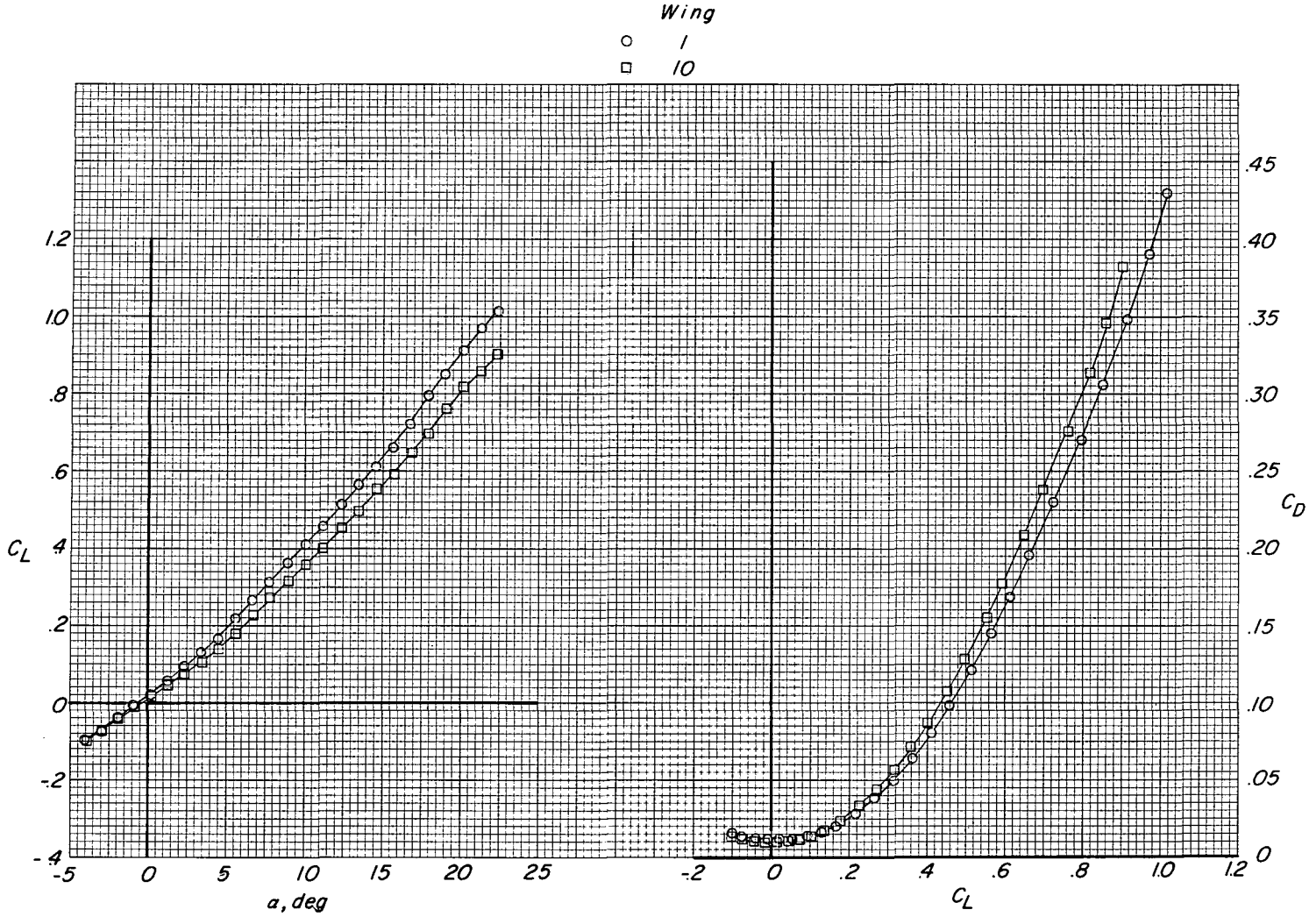

Figure 14.- Effect of wing planform on longitudinal aerodynamic characteristics of configurations with modified fuselage nose. Engine nacelles off; wings 1 and 10.

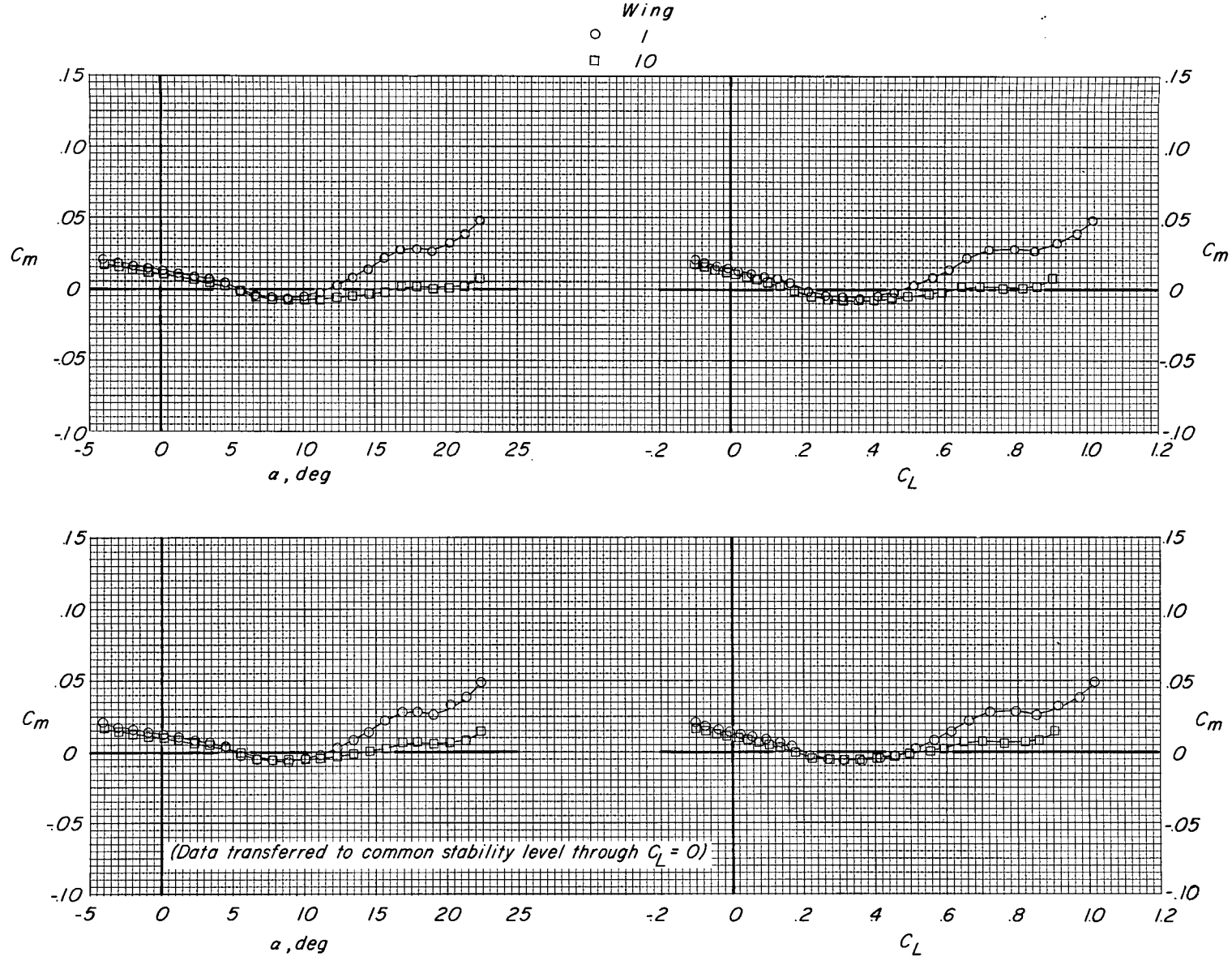

Figure 14.- Continued.

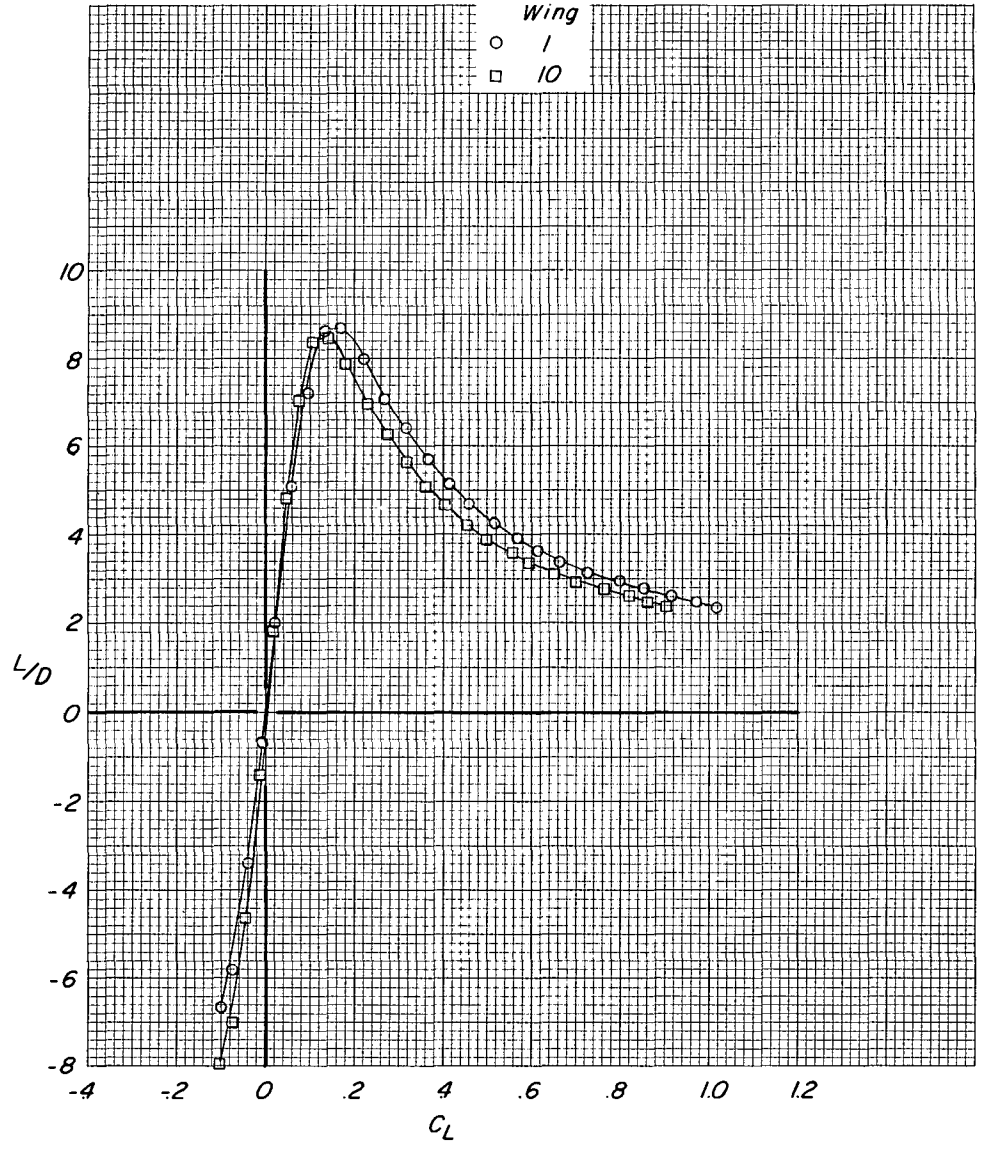

Figure 14.- Concluded.

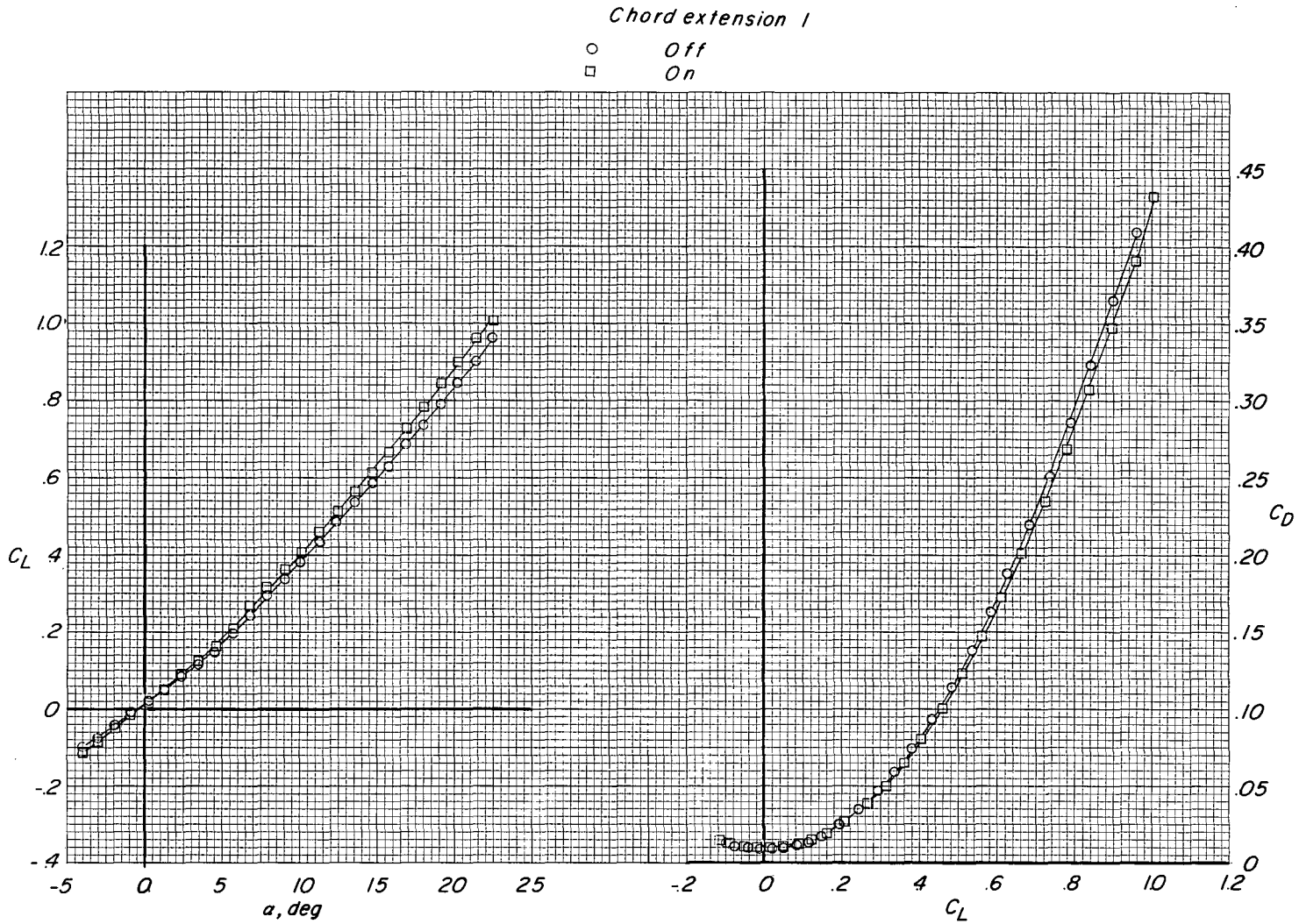

Figure 15.- Effect of wing leading-edge chord extension 1 on longitudinal aerodynamic characteristics of configuration with modified fuselage nose and wing 7. Engine nacelles off.

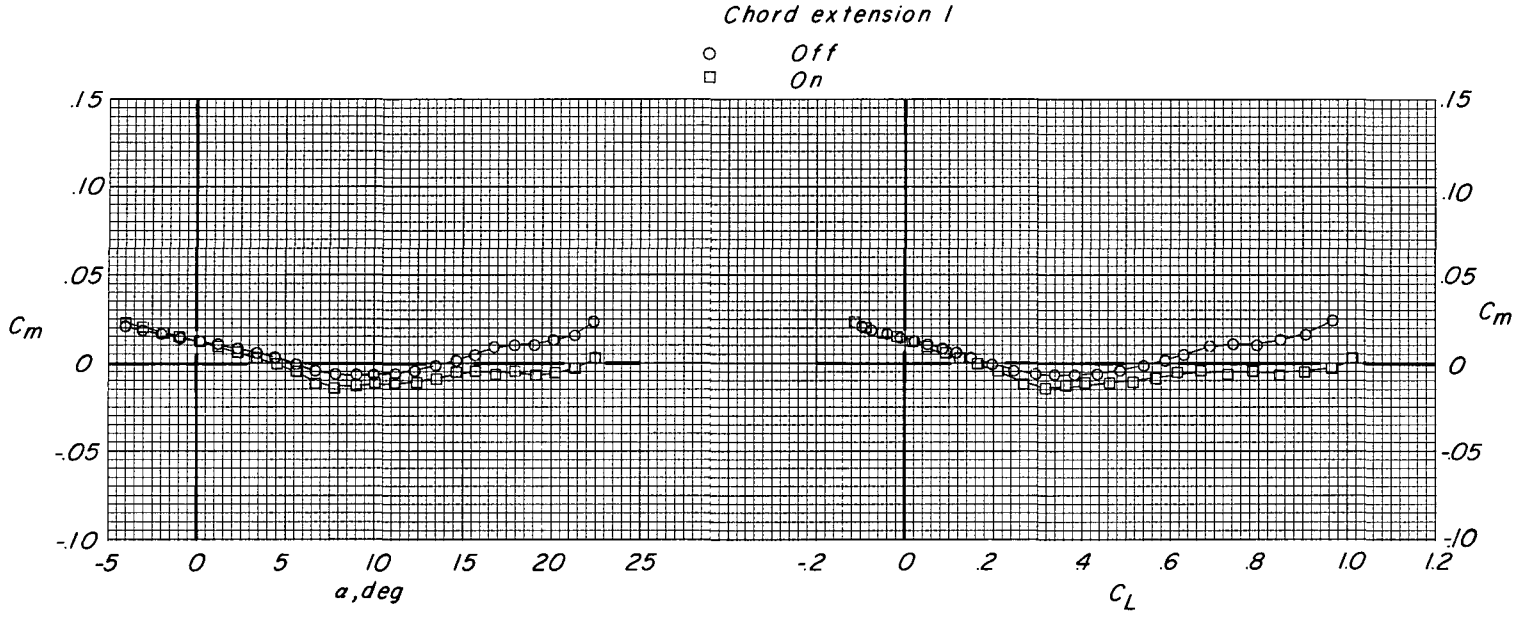

Figure 15.- Continued.

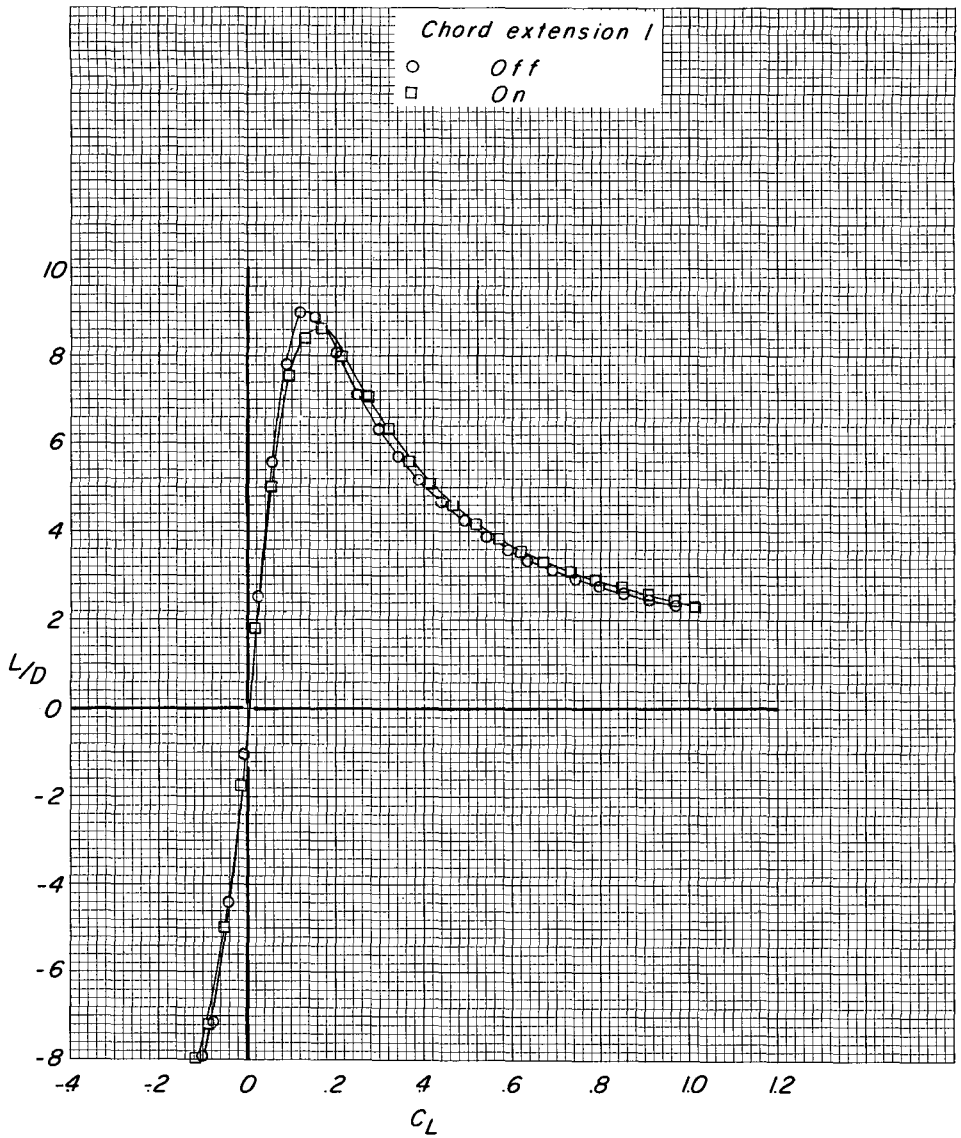

Figure 15.- Concluded.

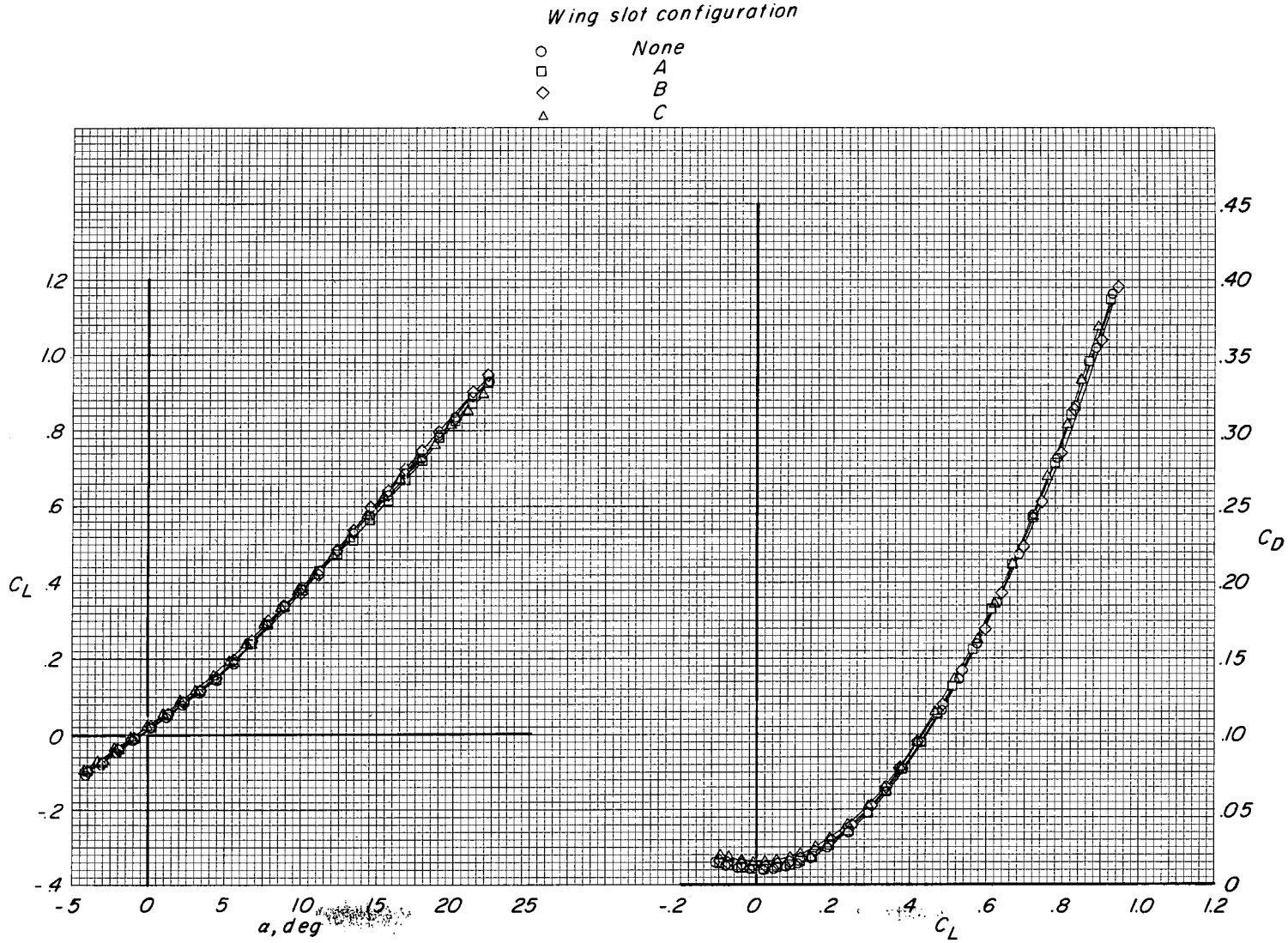

Figure 16.- Effect of slots in forward portion of wing on longitudinal aerodynamic characteristics of configuration with modified fuselage nose and wing 7. Engine nacelles off.

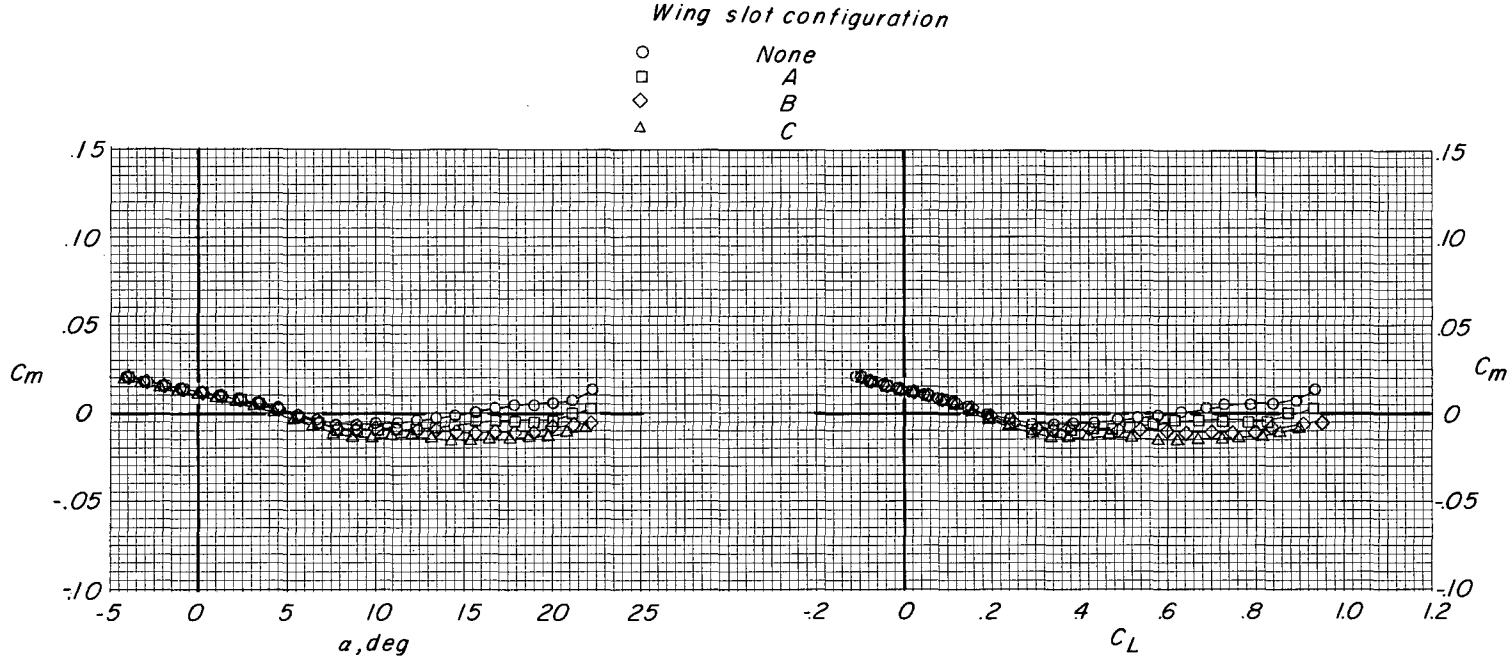

Figure 16.- Continued.

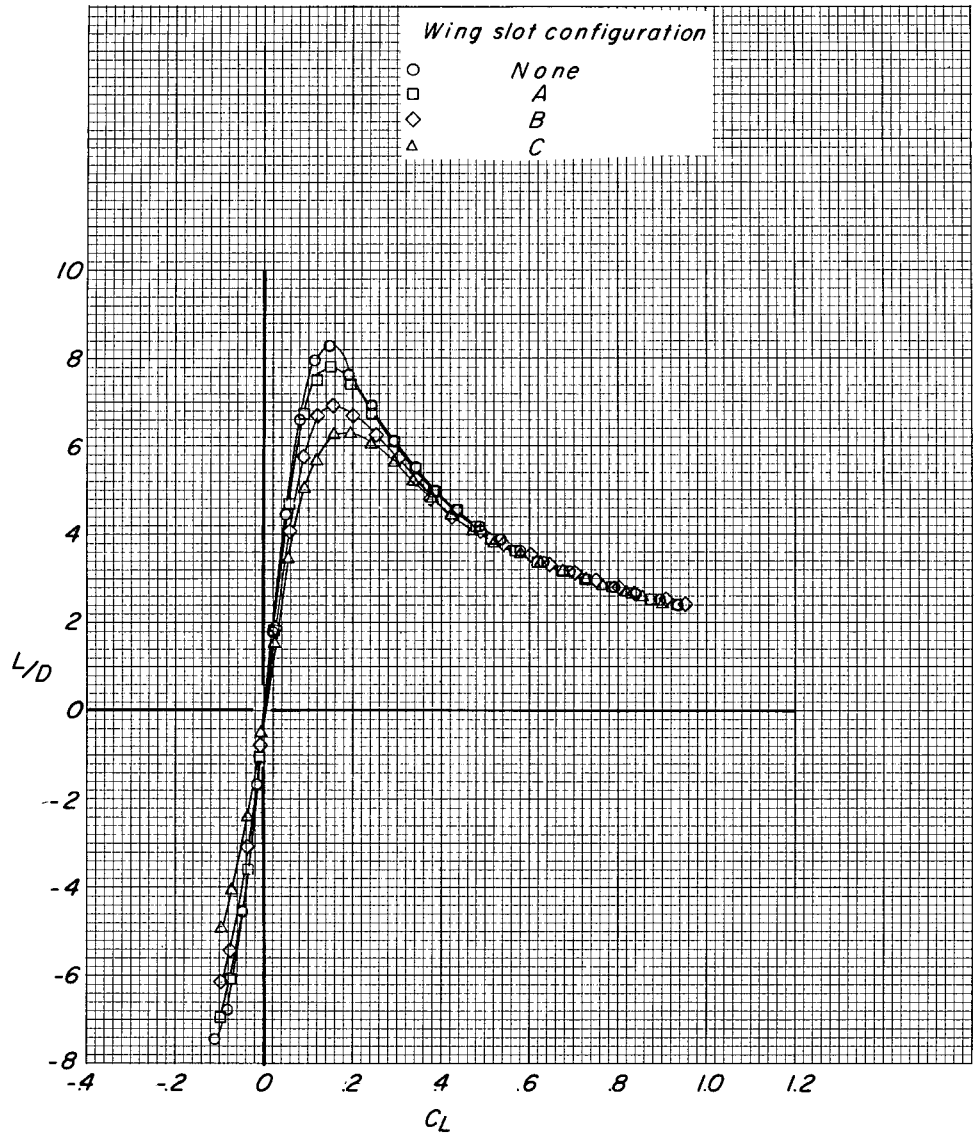

Figure 16.- Concluded.

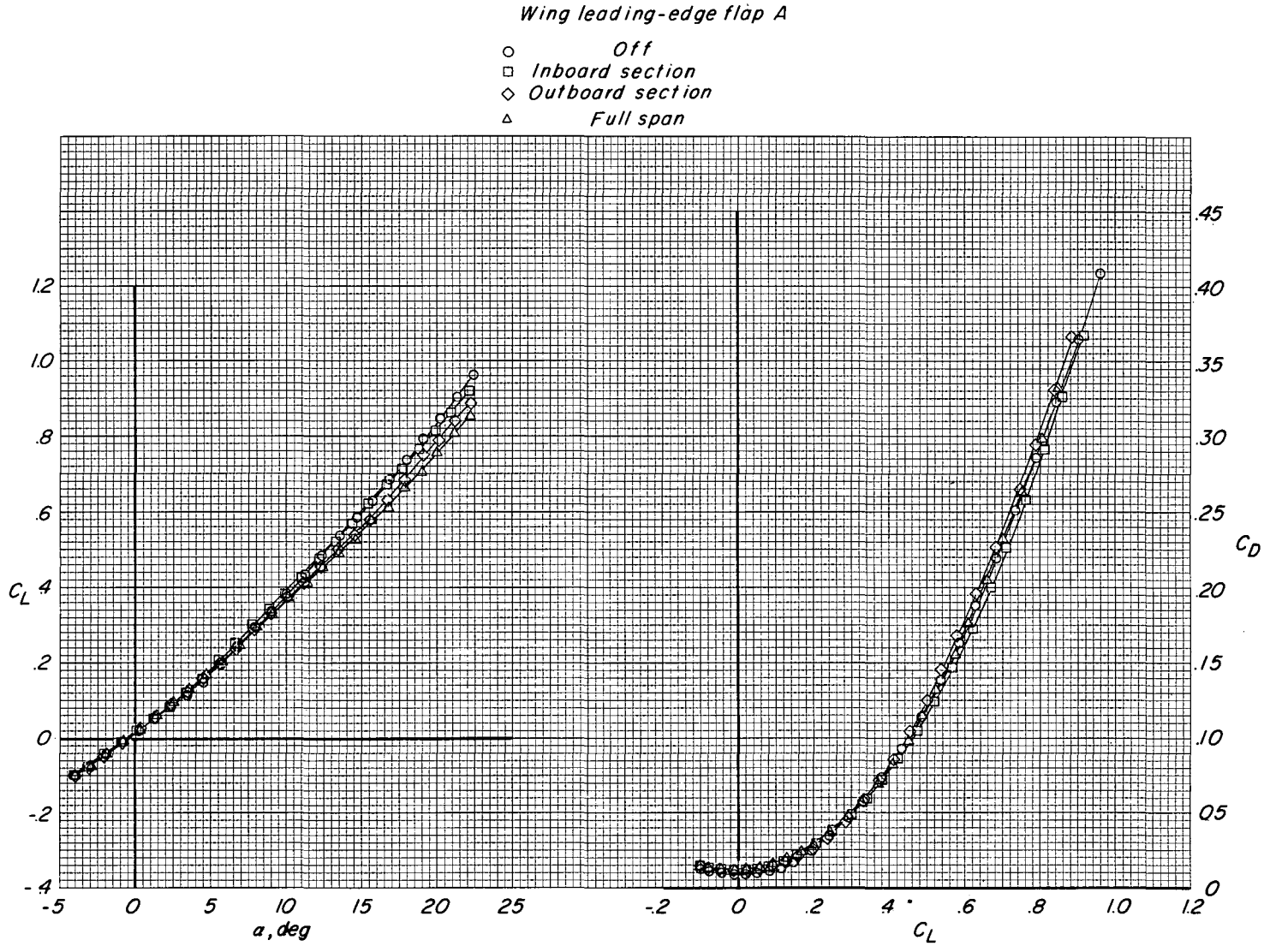

Figure 17.- Effect of leading-edge flap A on longitudinal aerodynamic characteristics of configuration with modified fuselage nose and wing 7. h = 0.45 in.; engine nacelles off.

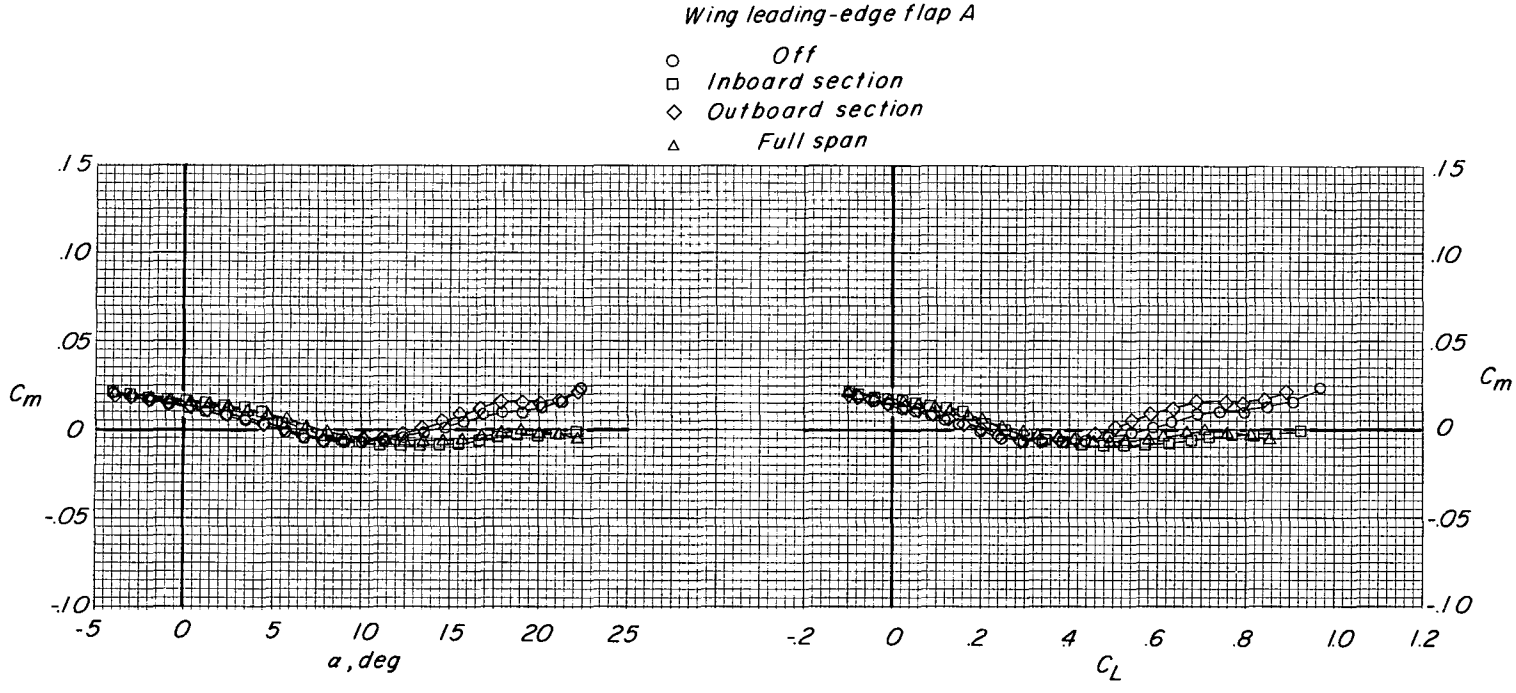

Figure 17.- Continued.

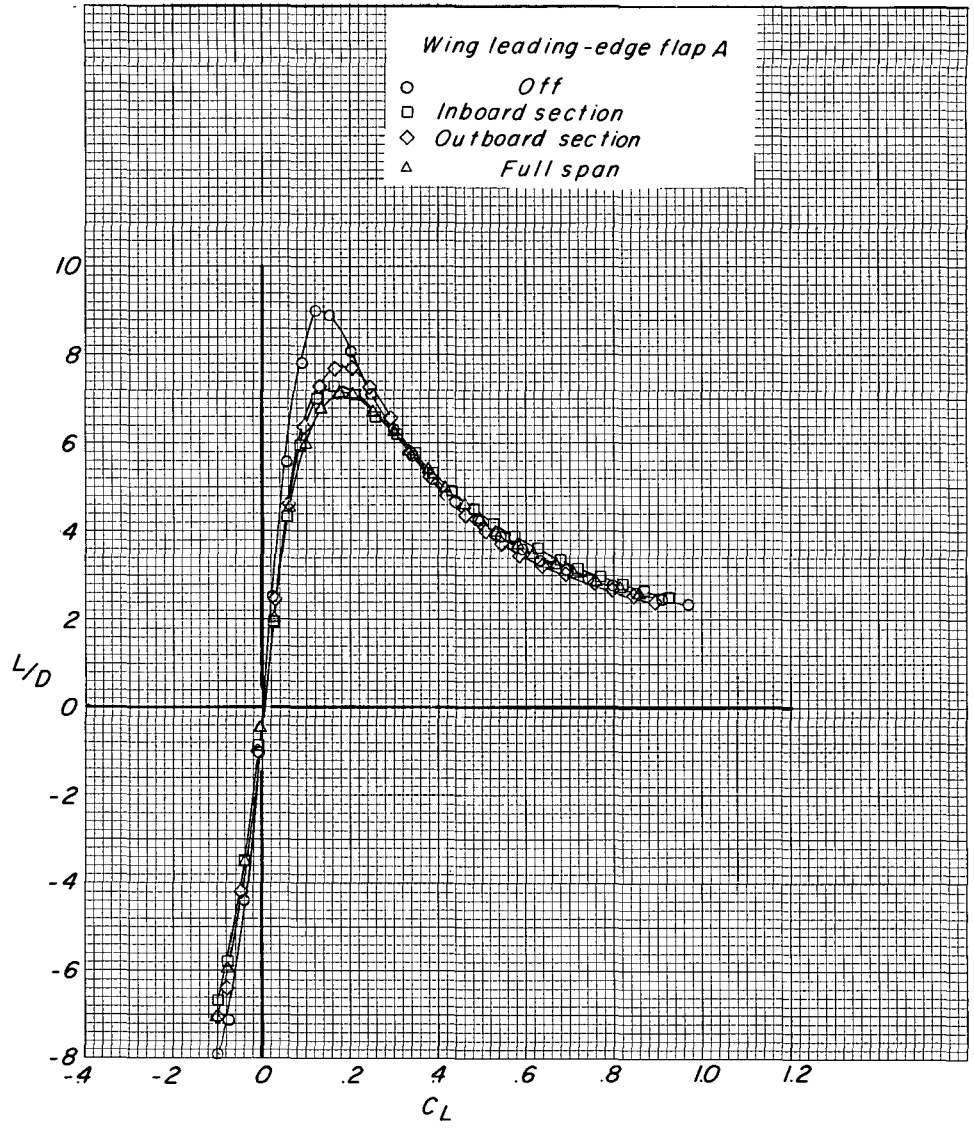

Figure 17.- Concluded.

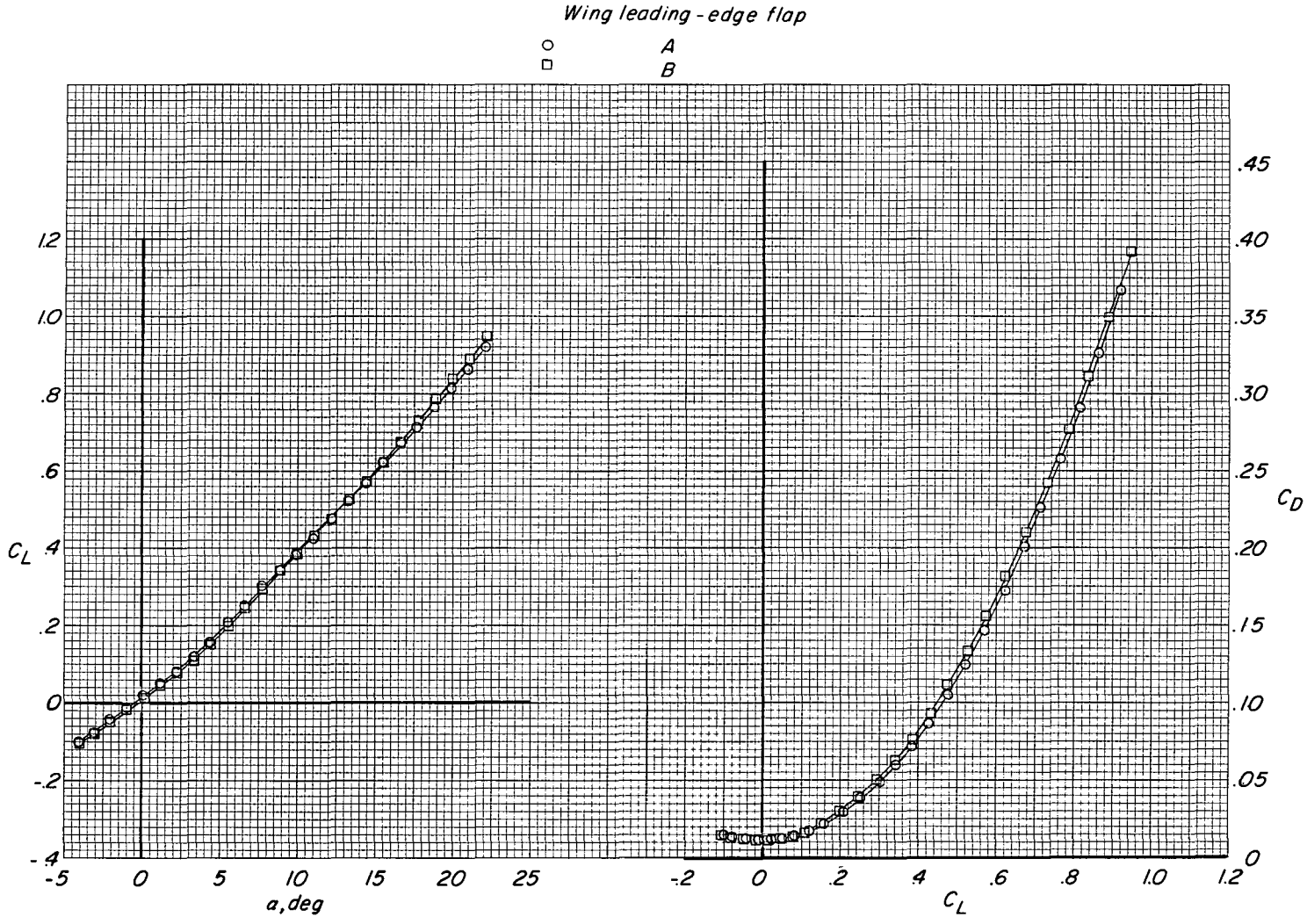

Figure 18.- Effect of inboard section of leading-edge flaps on longitudinal aerodynamic characteristics of configuration with modified fuselage nose and wing 7. h = 0.45 in.; engine nacelles off.

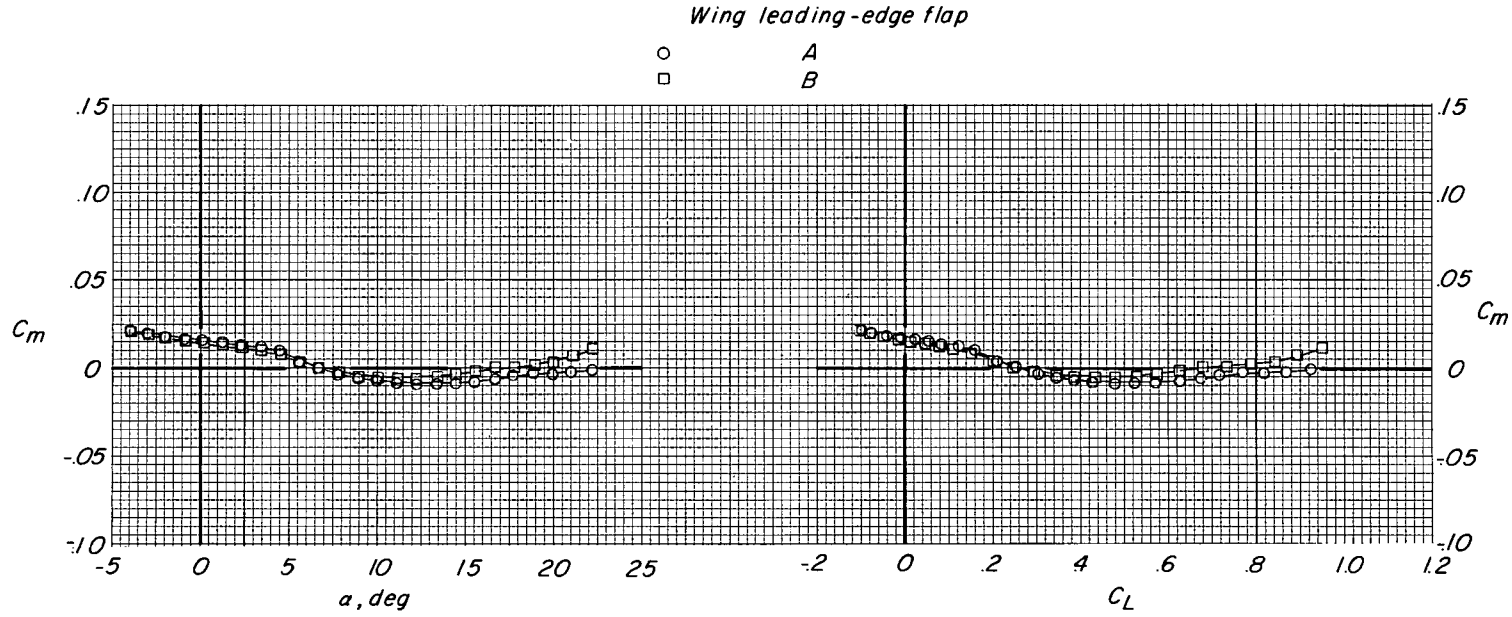

Figure 18.- Continued.

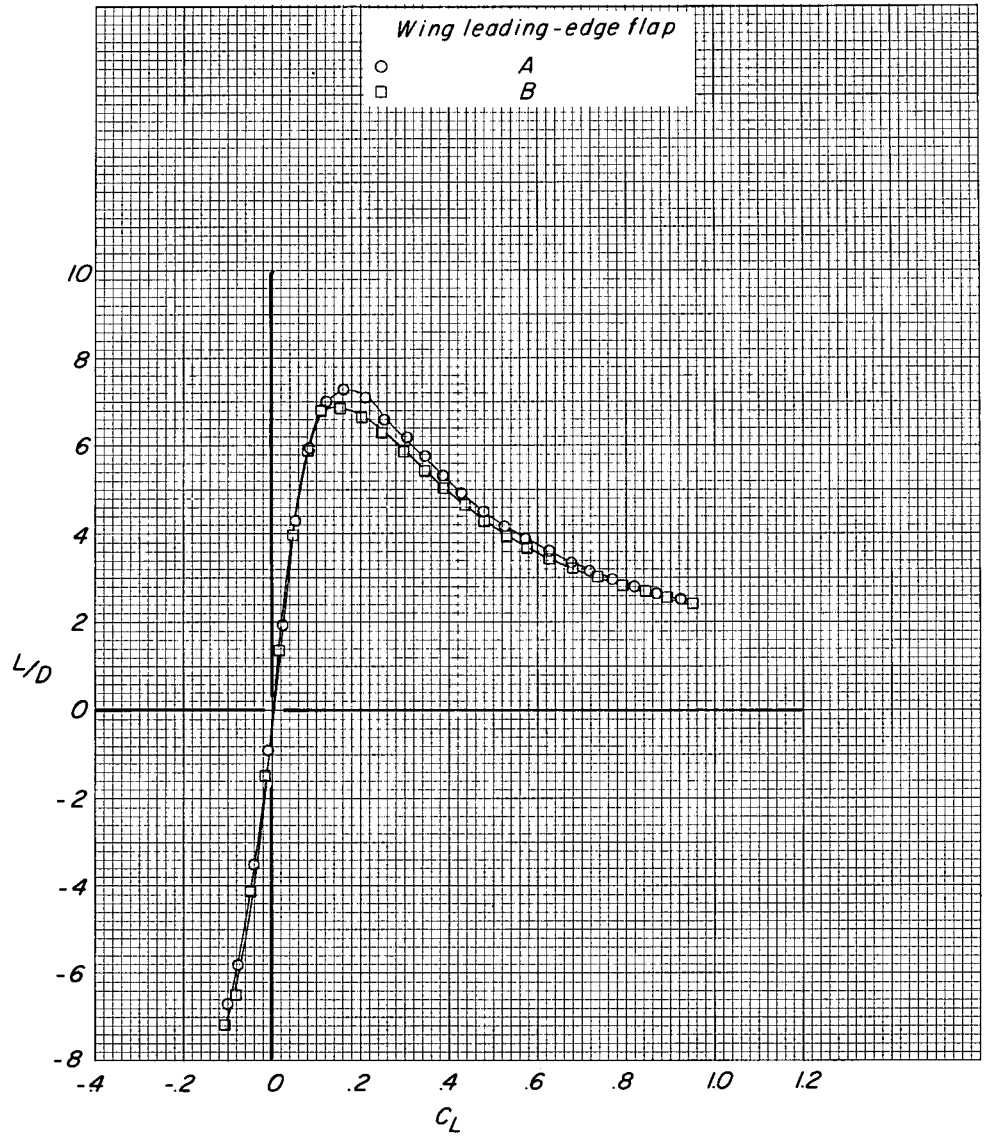

Figure 18.- Concluded.

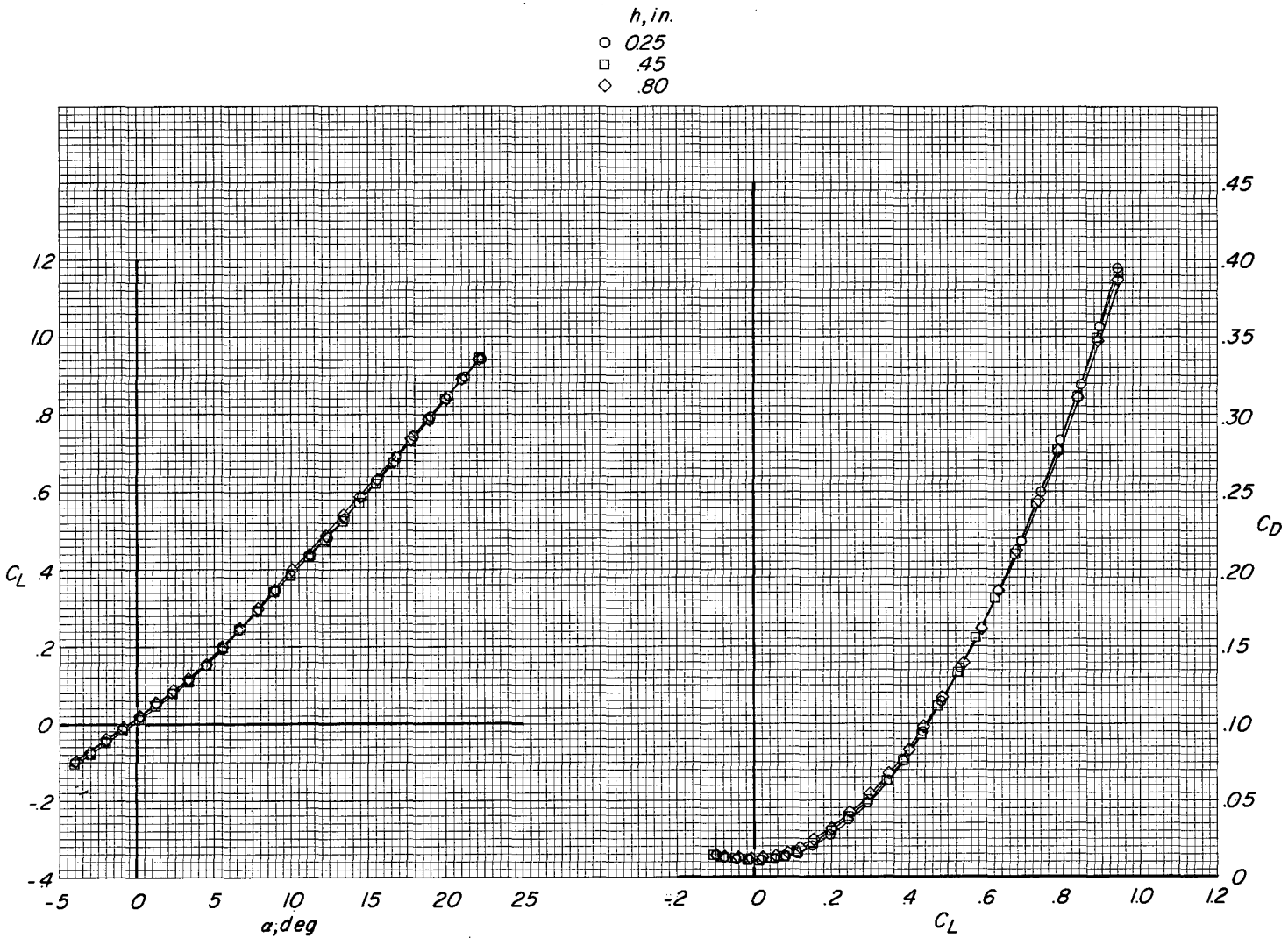

Figure 19.- Effect of height of inboard section of wing leading-edge flap B on longitudinal aerodynamic characteristics of configuration with modified fuselage nose and wing 7. Engine nacelles off.

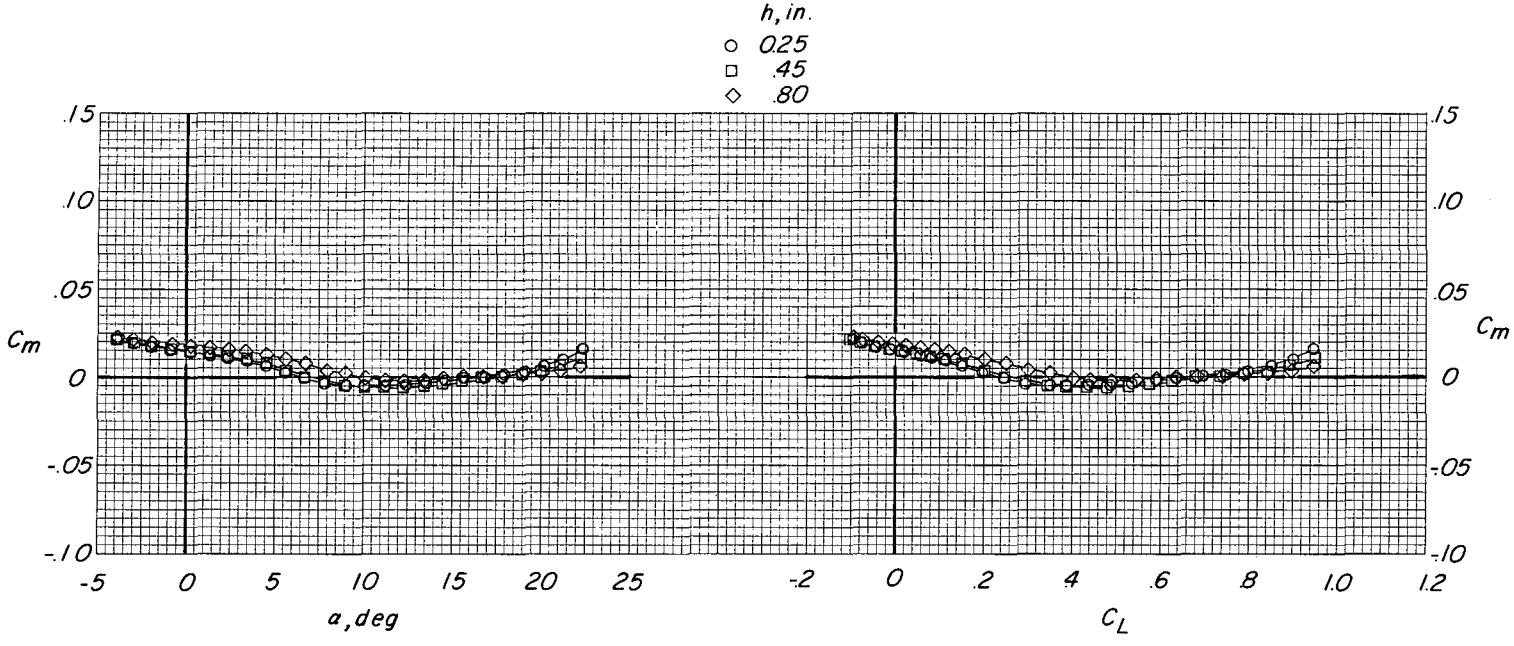

Figure 19.- Continued.

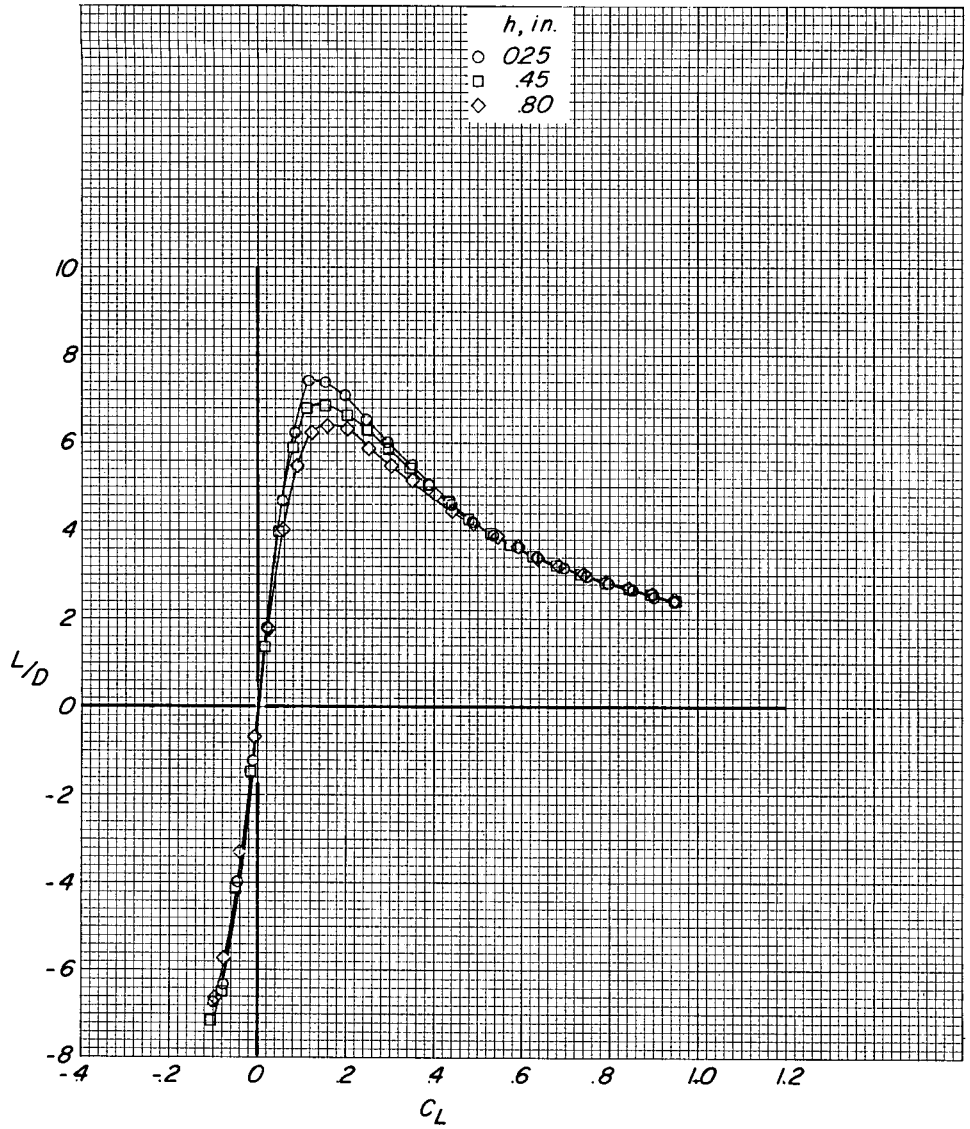

Figure 19.- Concluded.

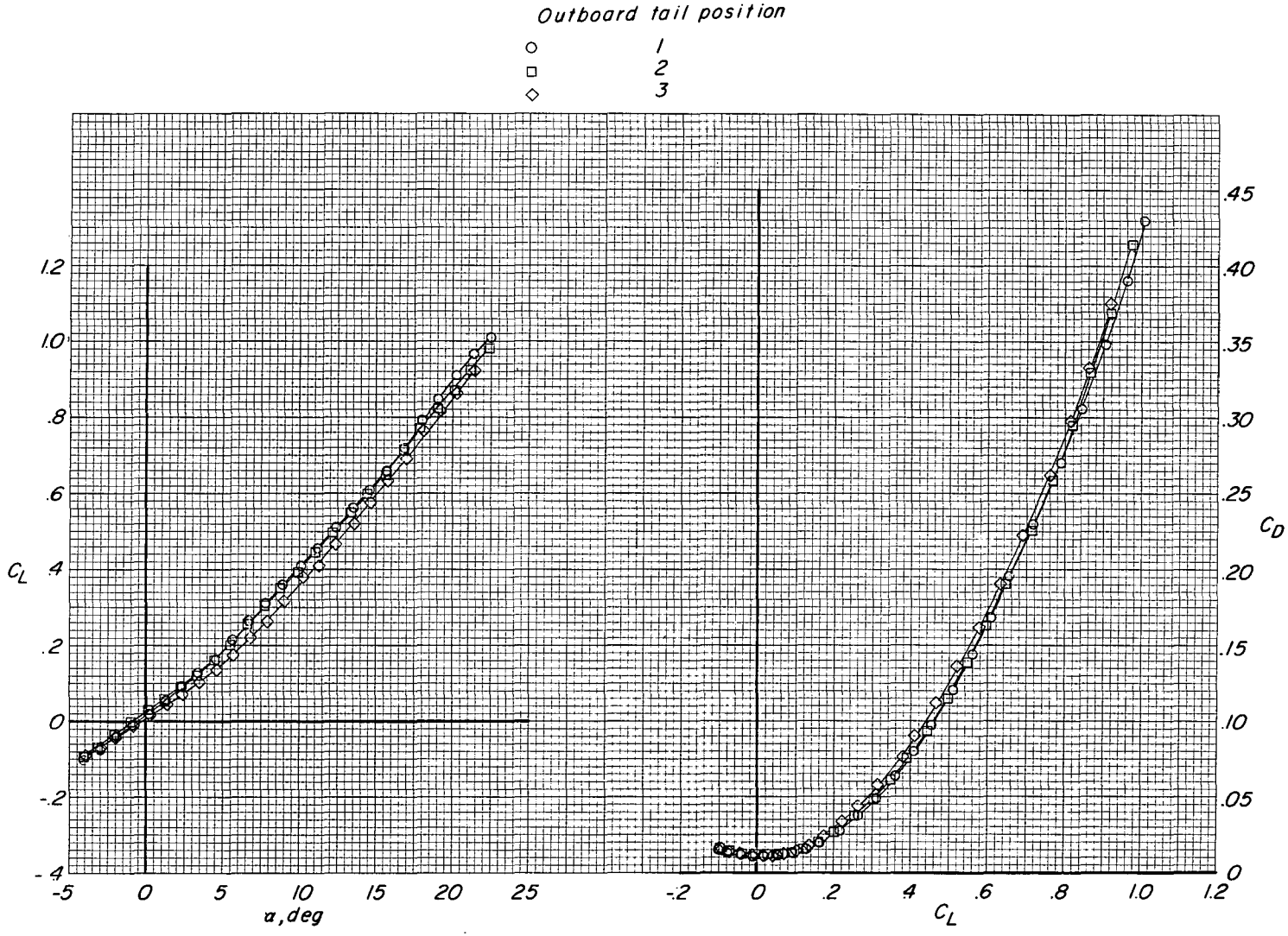

Figure 20.- Effect of position of outboard tails on longitudinal aerodynamic characteristics of configuration with modified fuselage nose and wing 1. Engine nacelles off.

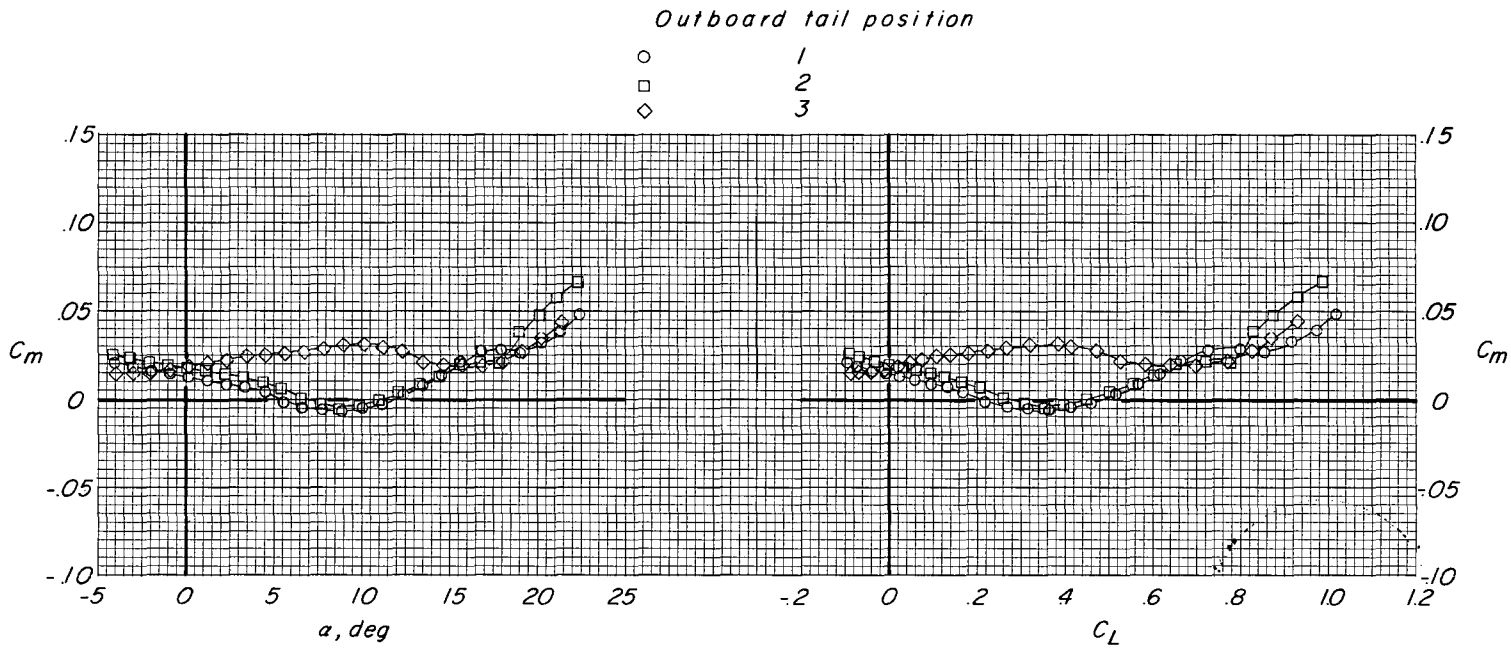

Figure 20.- Continued.

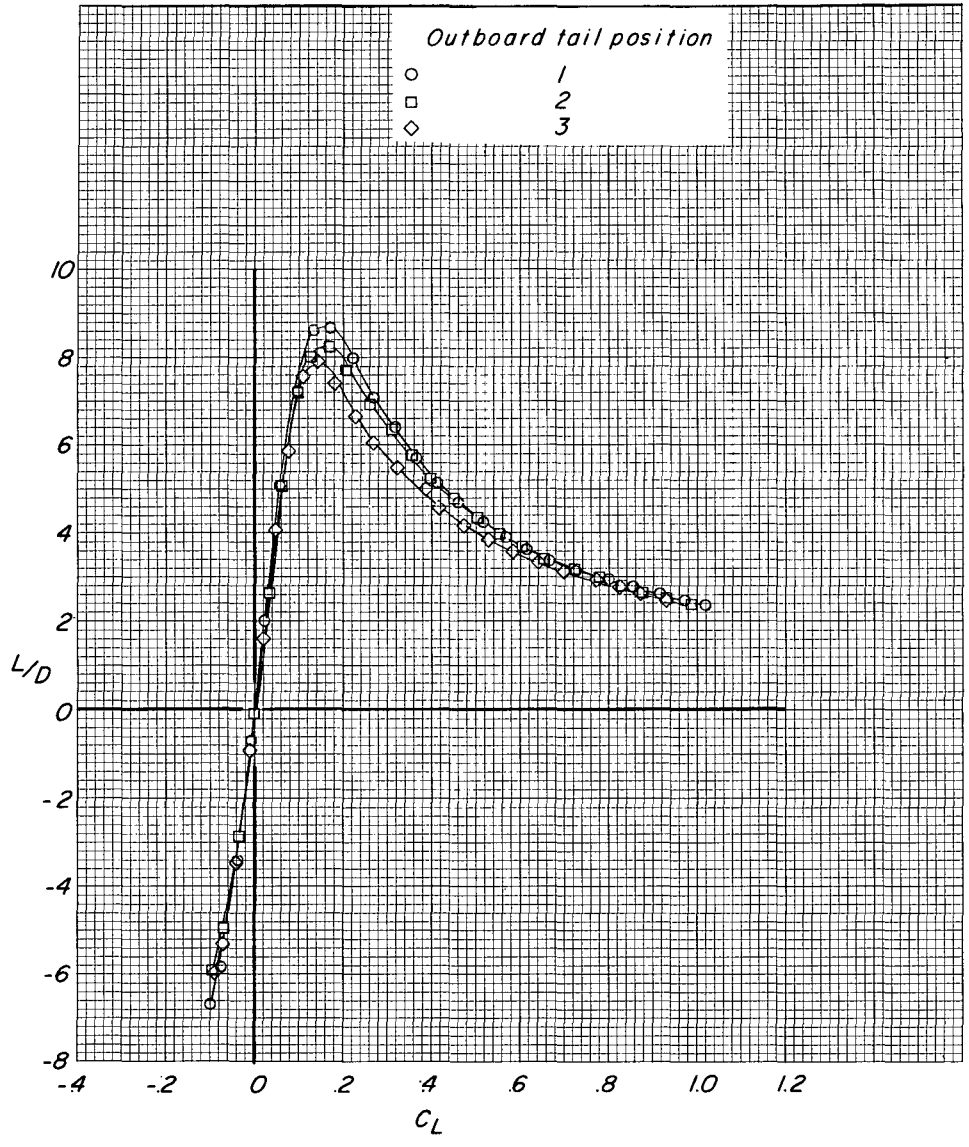

Figure 20.- Concluded.

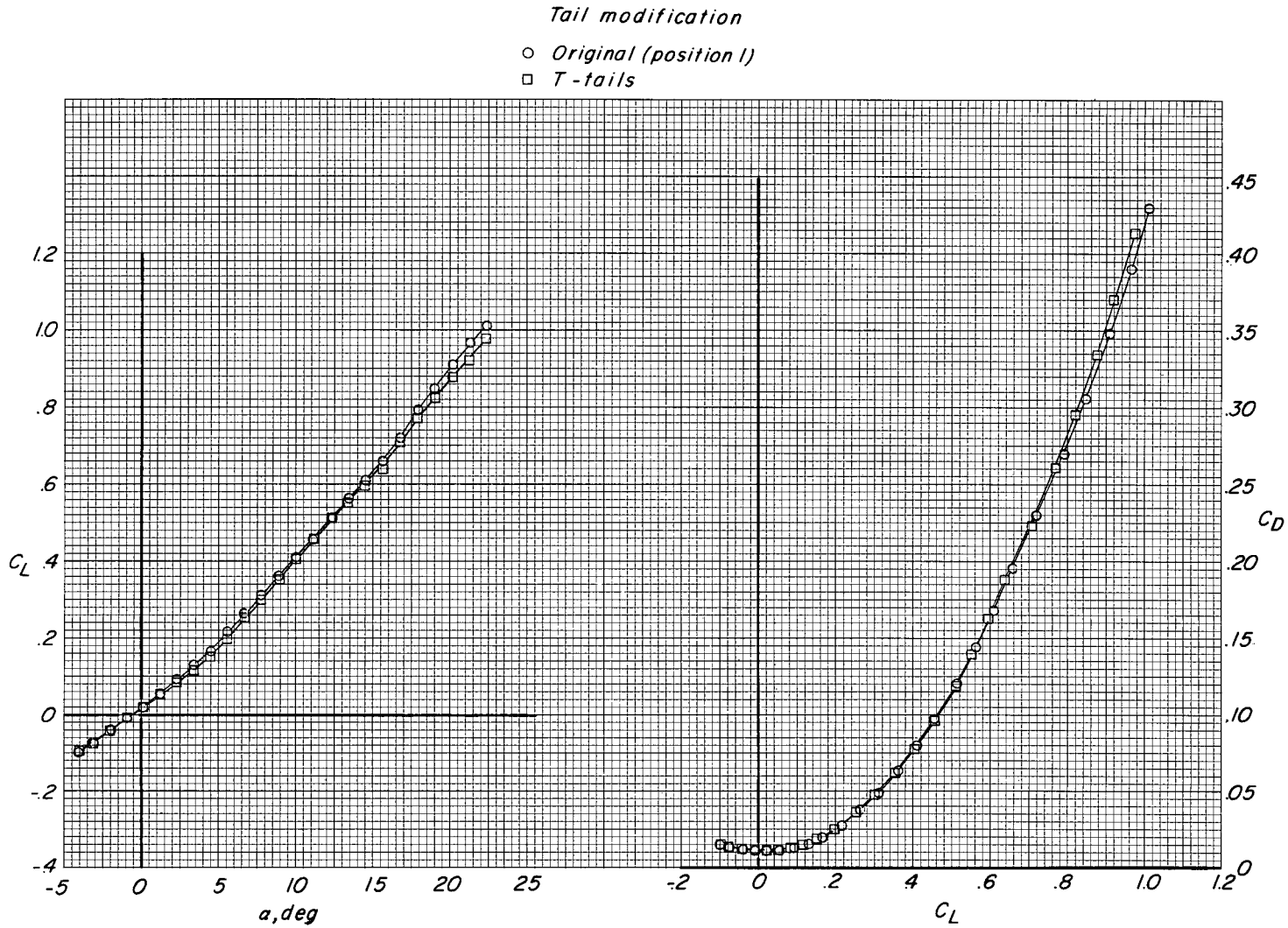

Figure 21.- Effect of tail modification on longitudinal aerodynamic characteristics of configuration with modified fuselage nose and wing 1. Engine nacelles off.

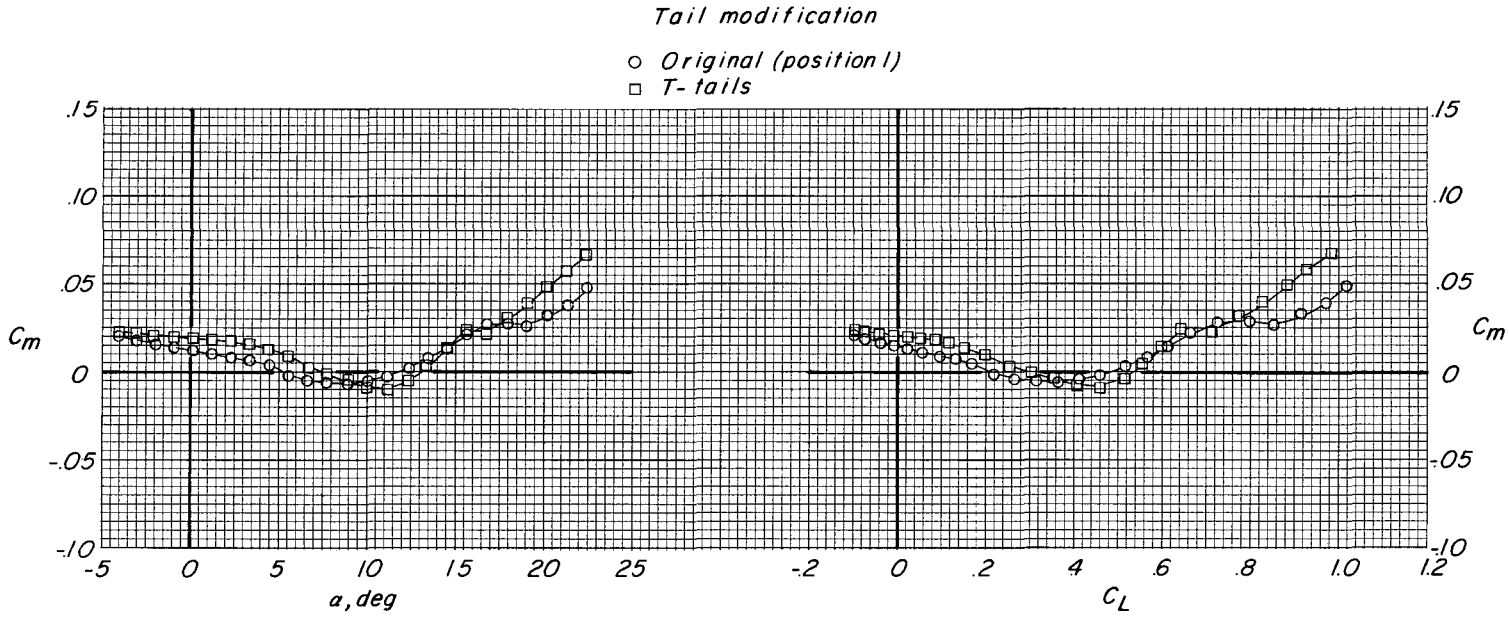

Figure 21.- Continued.

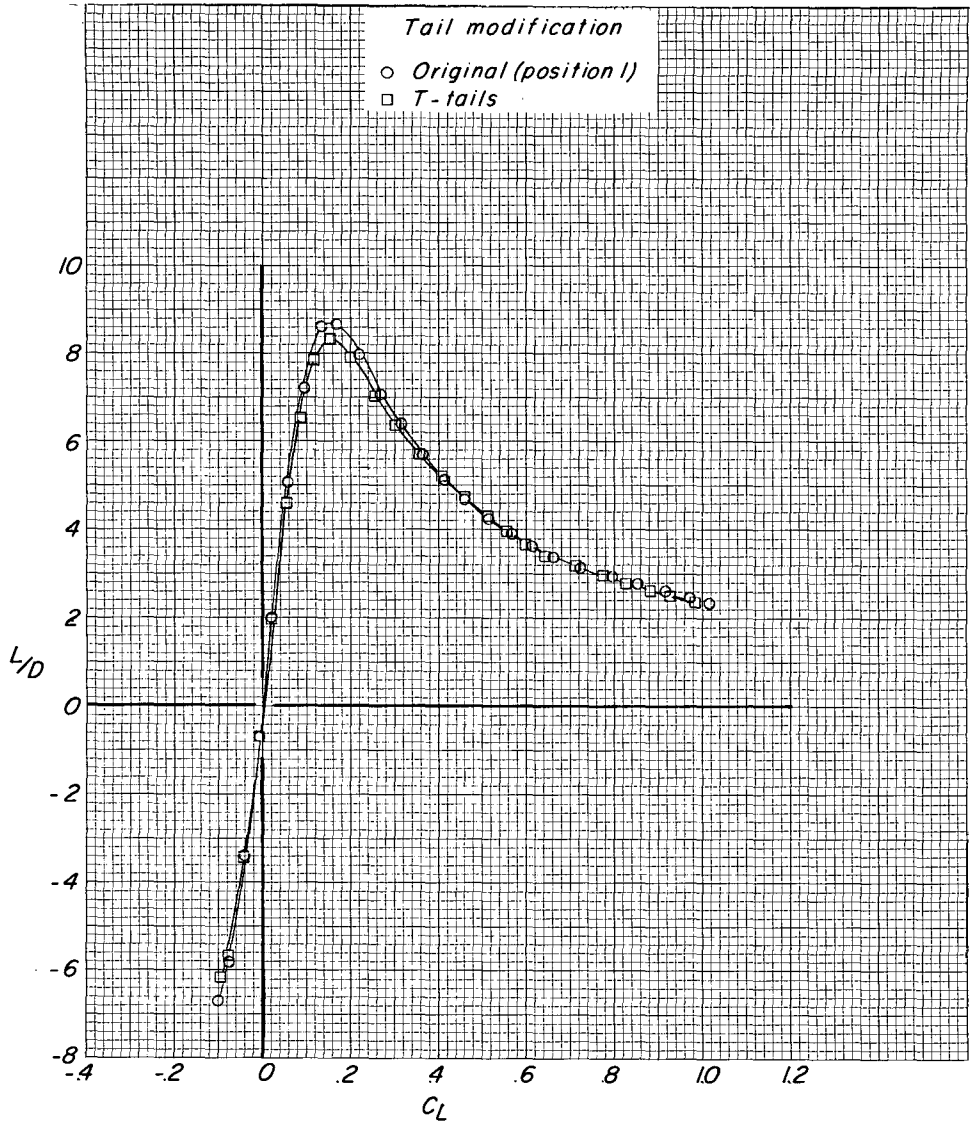

Figure 21.- Concluded.

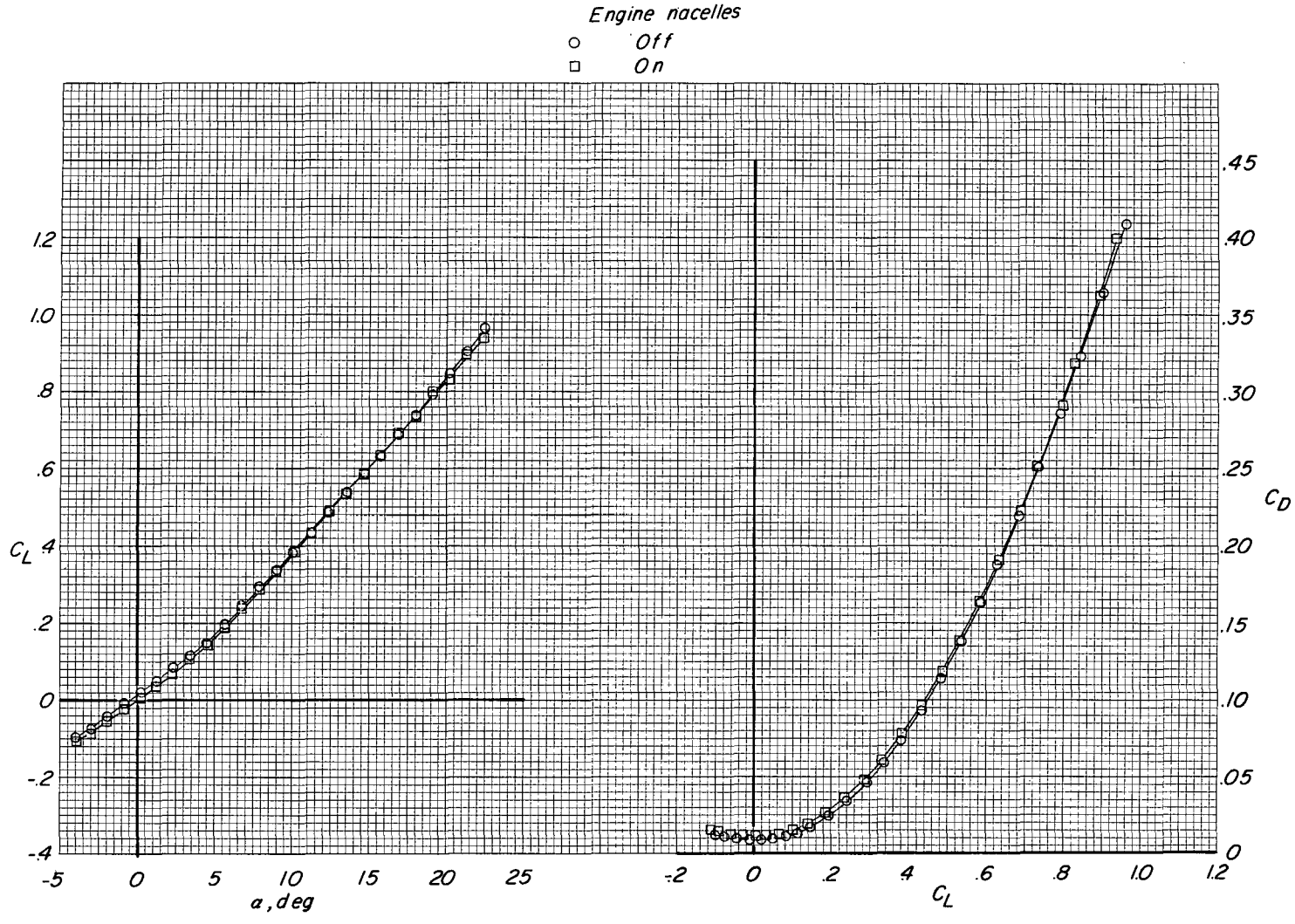

Figure 22.- Effect of engine nacelles on longitudinal aerodynamic characteristics of configuration with modified fuselage nose and wing 7.

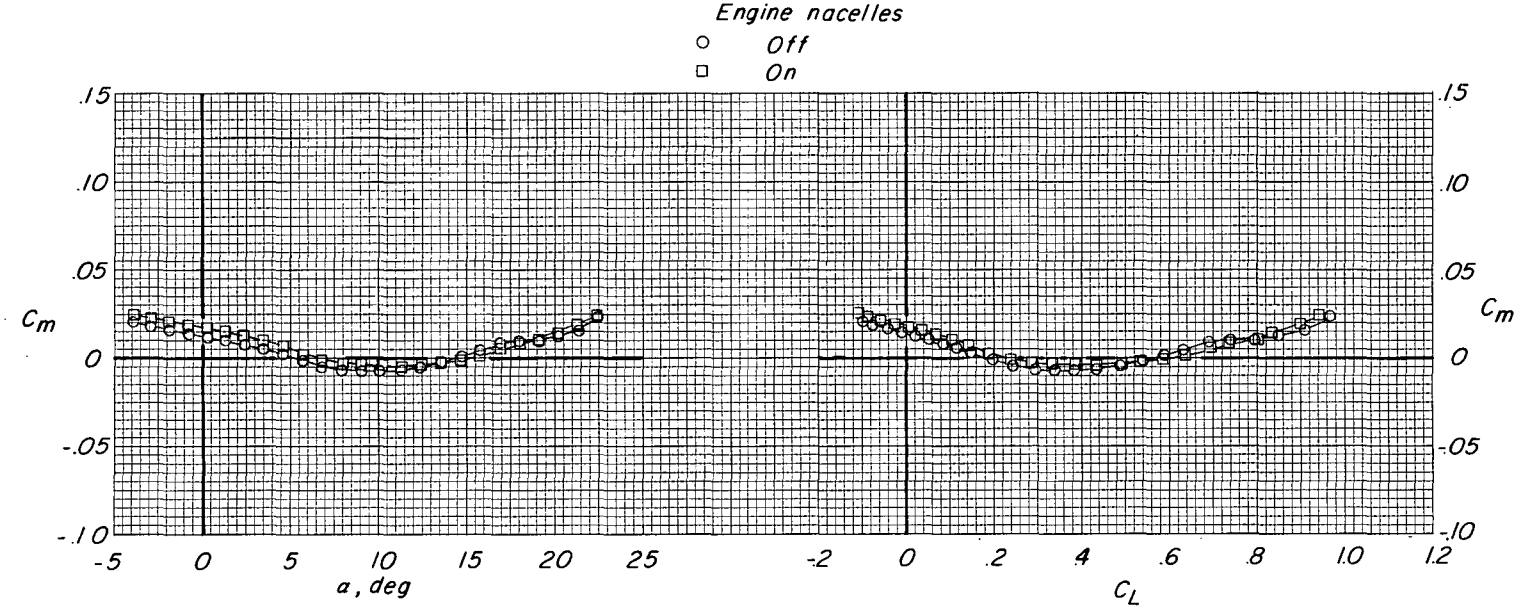

Figure 22.- Continued.

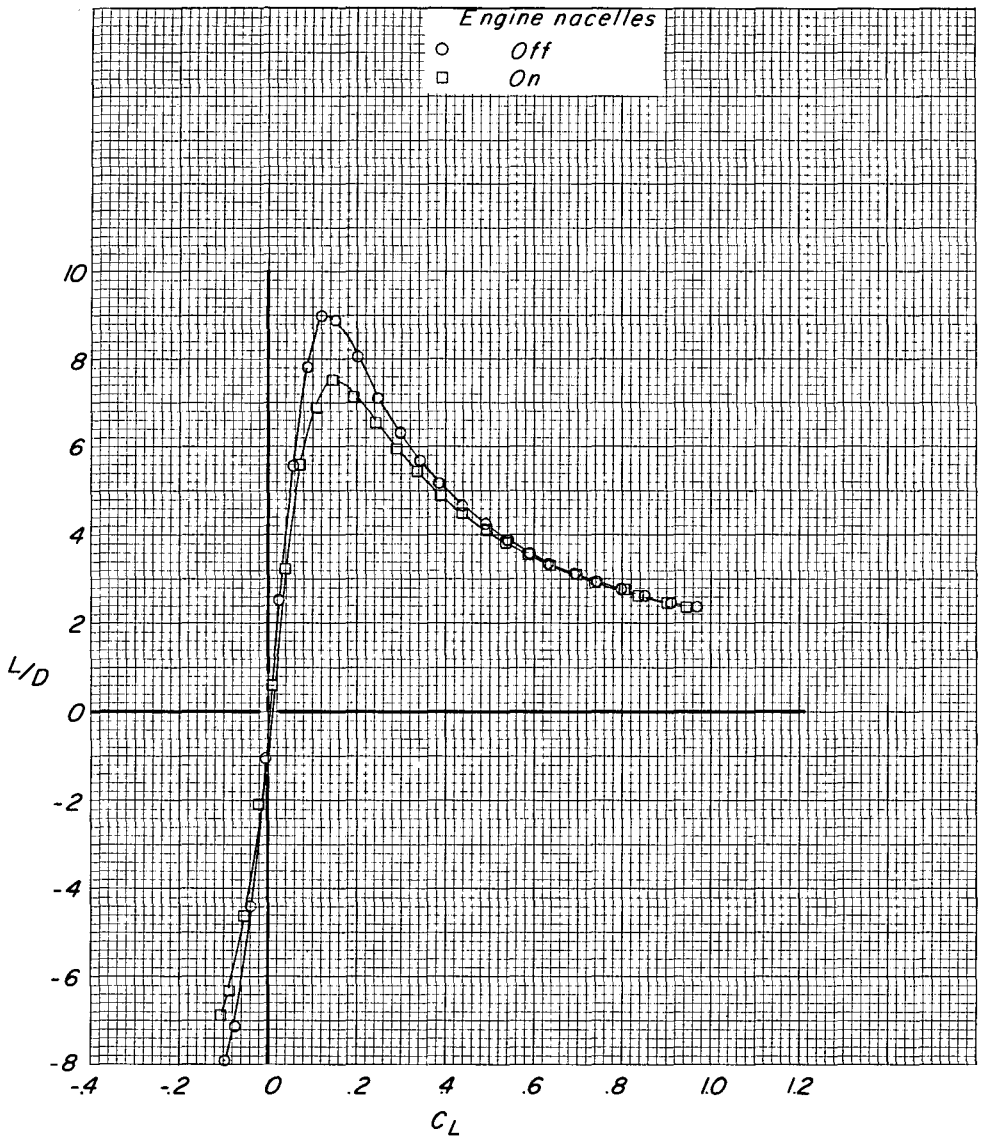

Figure 22.- Concluded.

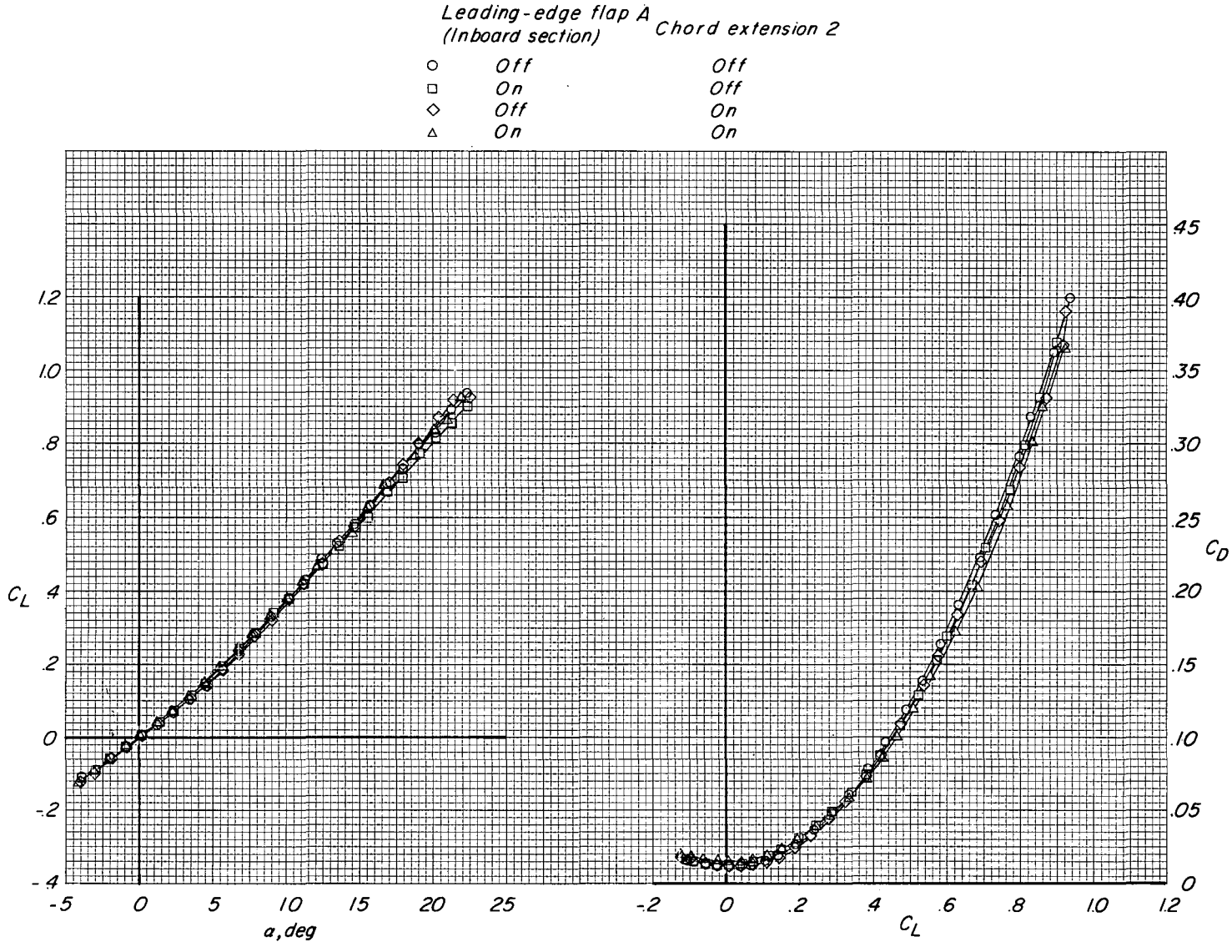

Figure 23.- Combined effect of leading-edge flaps and chord extensions on longitudinal aerodynamic characteristics of configuration with modified fuselage nose and wing 7. Engine nacelle on.

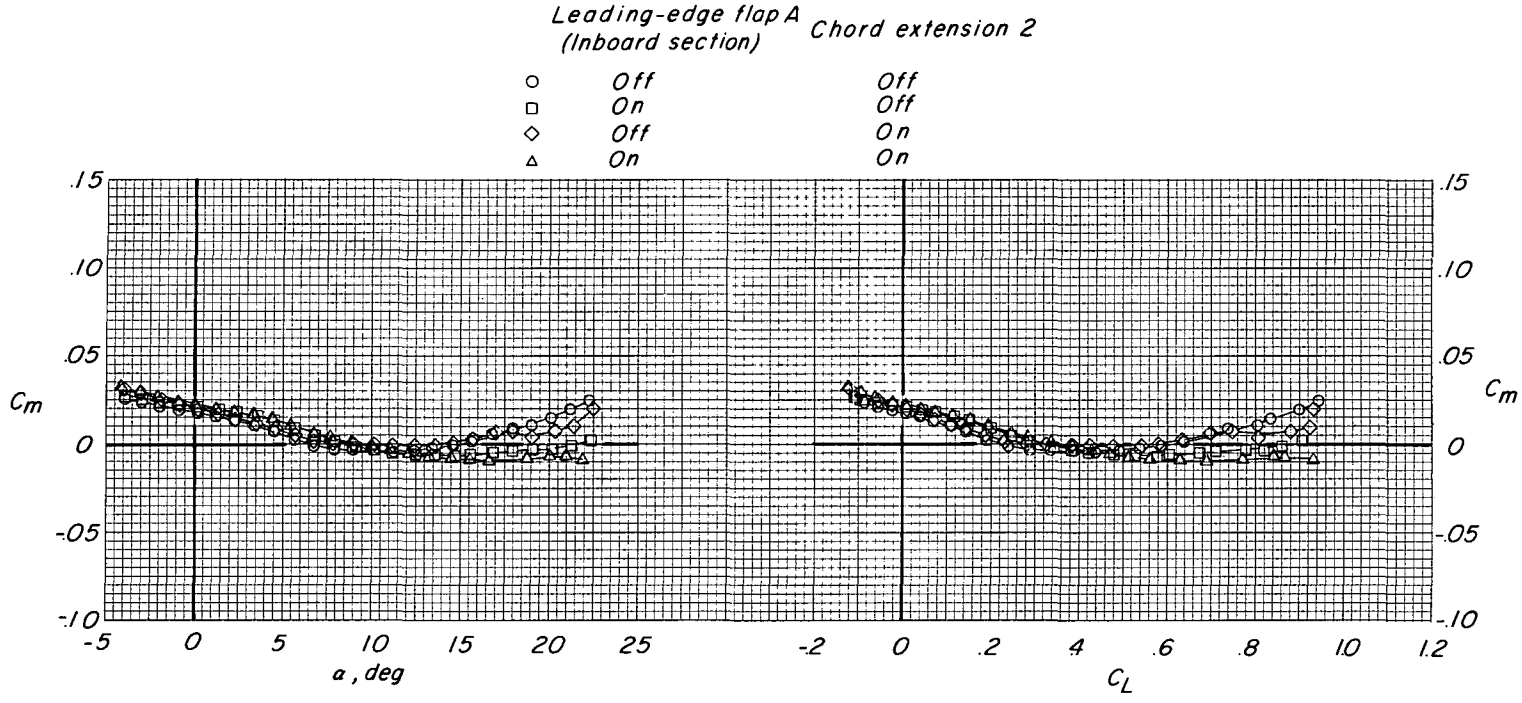

Figure 23.- Continued.

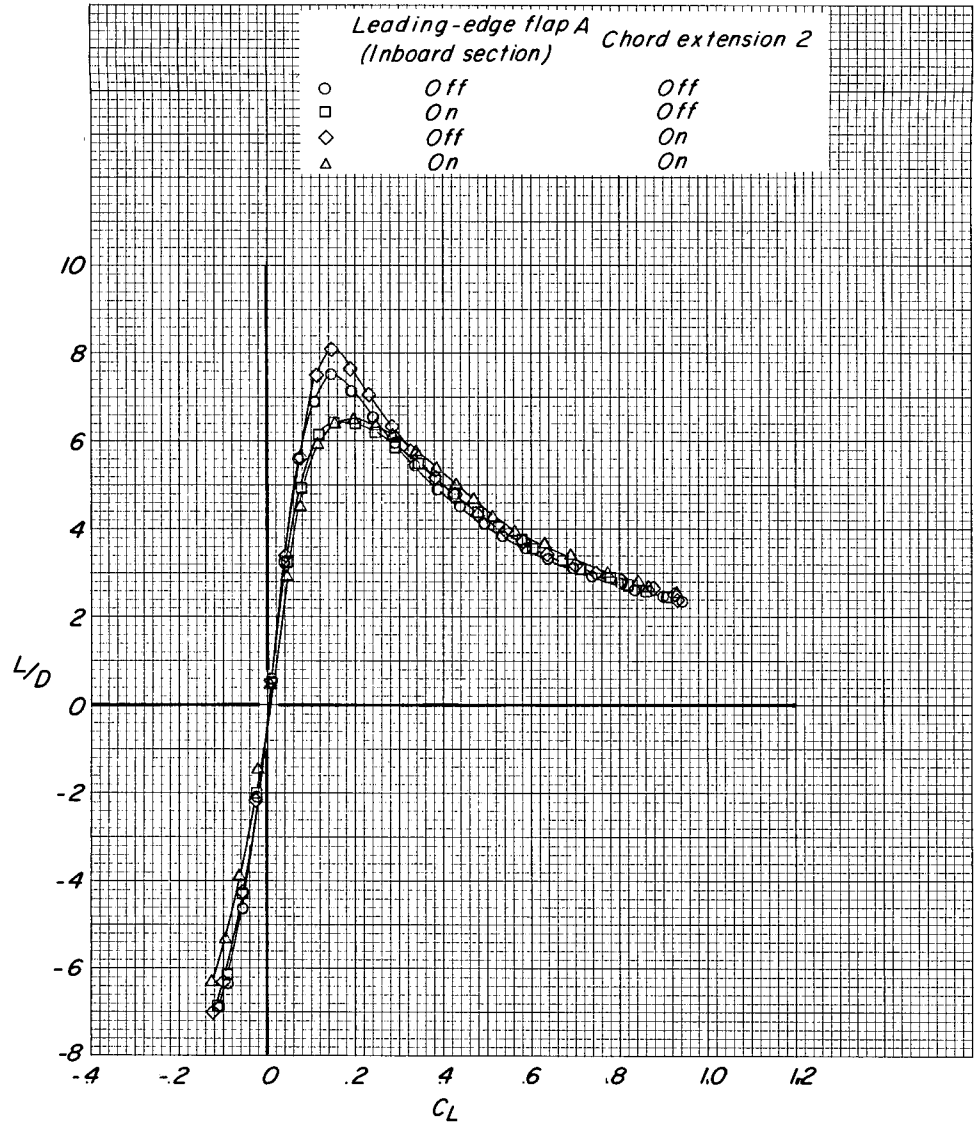

Figure 23.- Concluded.

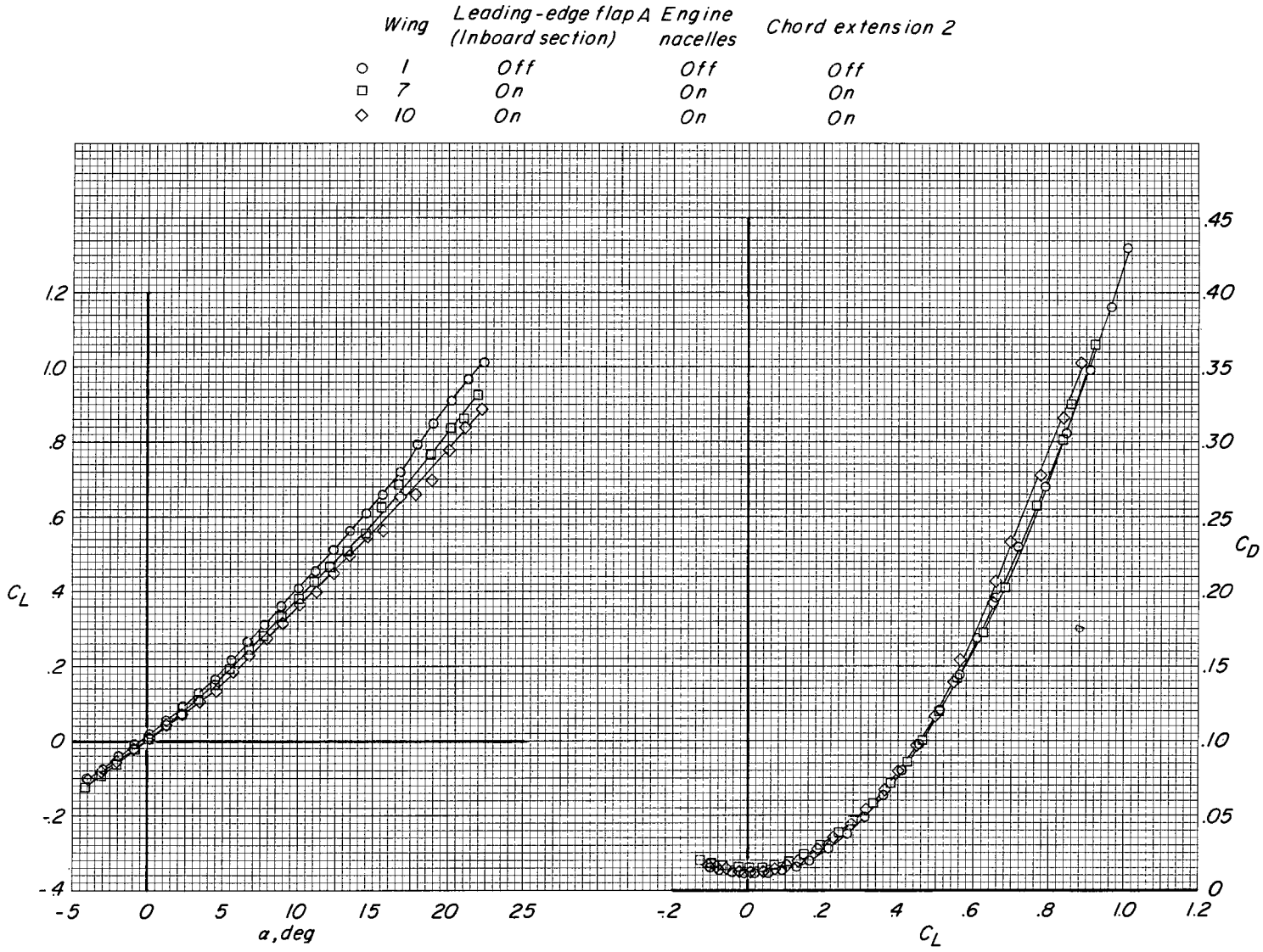

Figure 24.- Combined effect of some of configuration modifications on longitudinal aerodynamic characteristics of configuration with modified fuselage nose.

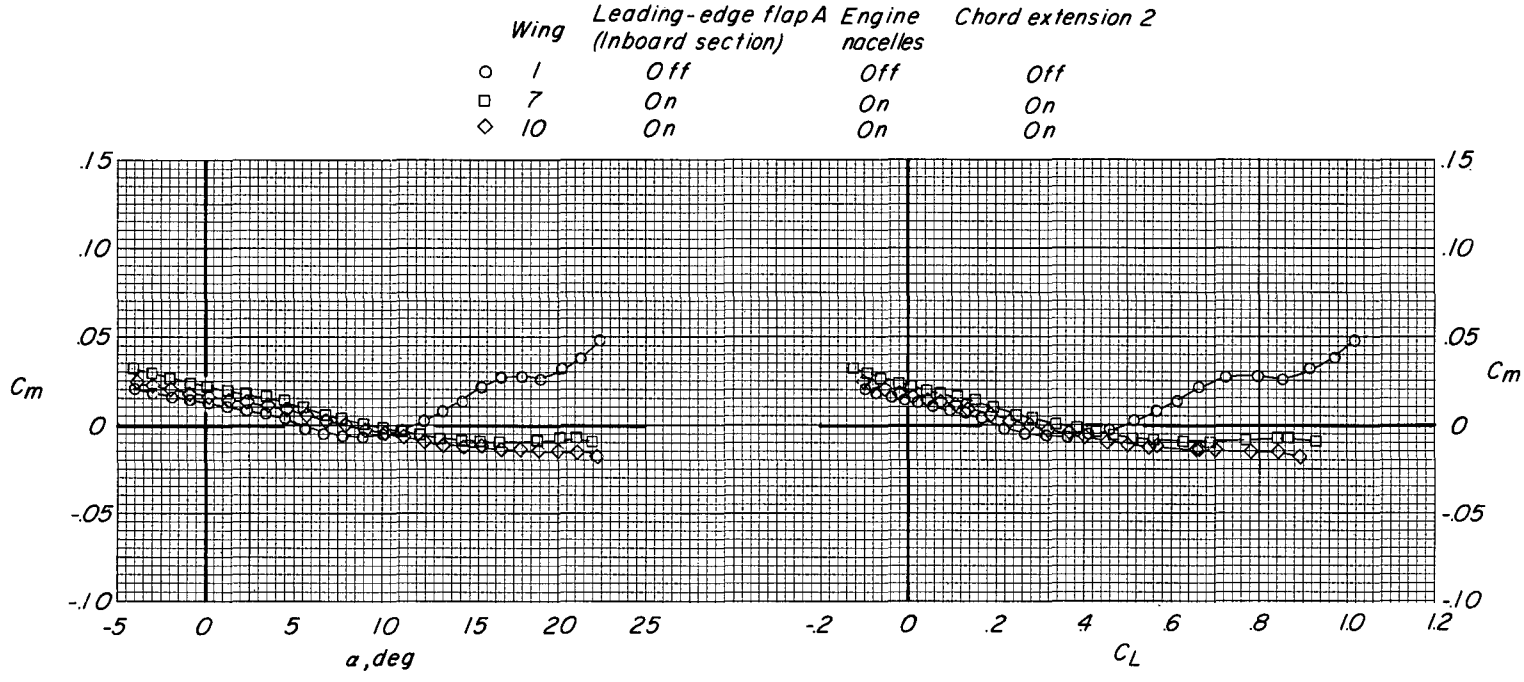

Figure 24.- Continued.

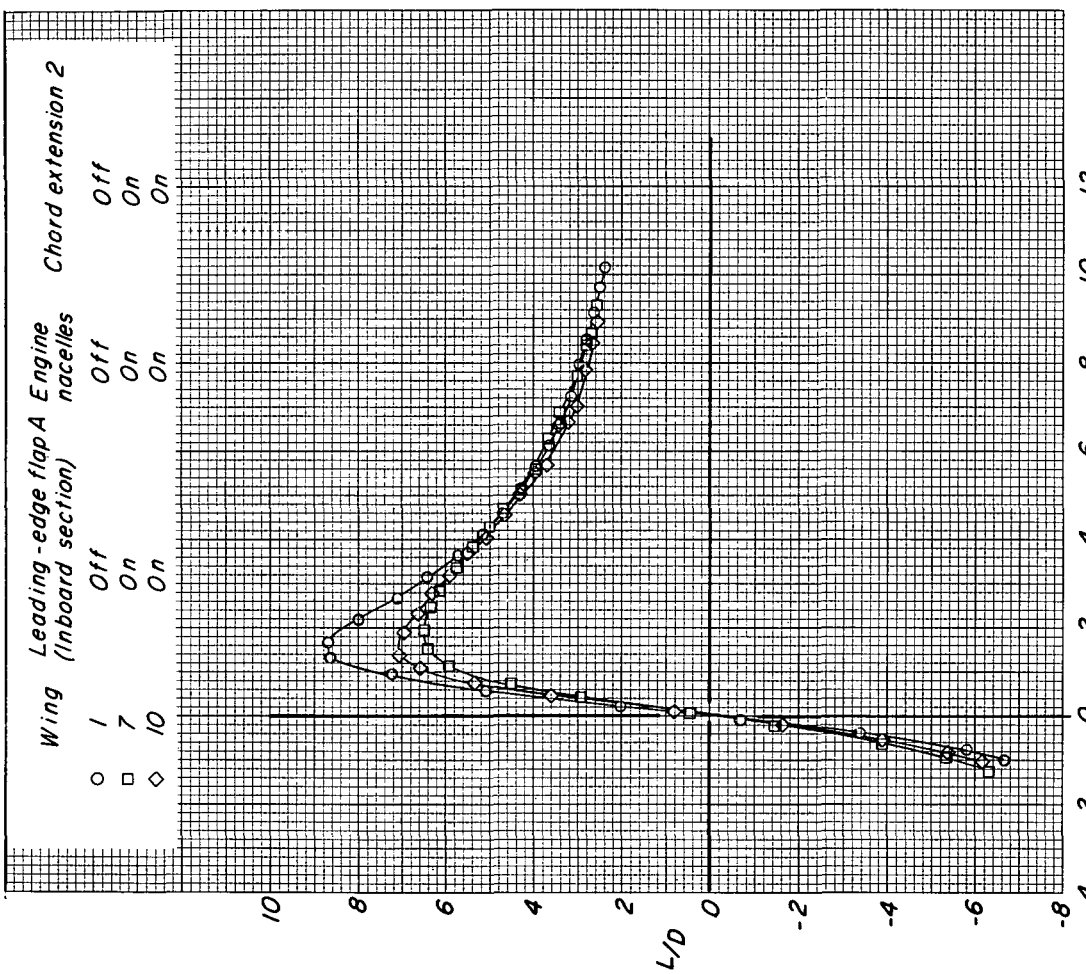

Figure 24.- Concluded.

NASA-Langley, 1965 L-4254